Composite particle theory of three-dimensional gapped fermionic phases: Fractional topological insulators and charge-loop excitation symmetry

Peng Ye,[1] Taylor L. Hughes,[1] Joseph Maciejko,[2,3,4] and Eduardo Fradkin[1]

[1]*Department of Physics and Institute for Condensed Matter Theory, University of Illinois at Urbana-Champaign, Illinois 61801, USA*

[2]*Department of Physics, University of Alberta, Edmonton, Alberta, Canada T6G 2E1*

[3]*Theoretical Physics Institute, University of Alberta, Edmonton, Alberta, Canada T6G 2E1*

[4]*Canadian Institute for Advanced Research, Toronto, Ontario, Canada M5G 1Z8*

(Received 24 March 2016; revised manuscript received 10 August 2016; published 2 September 2016)

Topological phases of matter are usually realized in deconfined phases of gauge theories. In this context, confined phases with strongly fluctuating gauge fields seem to be irrelevant to the physics of topological phases. For example, the low-energy theory of the two-dimensional (2D) toric code model (i.e., the deconfined phase of $\mathbb{Z}_2$ gauge theory) is a U(1) × U(1) Chern-Simons theory in which gauge charges (i.e., e and m particles) are deconfined and the gauge fields are gapped, while the confined phase is topologically trivial. In this paper, we point out a route to constructing exotic three-dimensional (3D) gapped fermionic phases in a confining phase of a gauge theory. Starting from a parton construction with strongly fluctuating compact U(1) × U(1) gauge fields, we construct gapped phases of interacting fermions by condensing two linearly independent bosonic composite particles consisting of partons and U(1) × U(1) magnetic monopoles. This can be regarded as a 3D generalization of the 2D Bais-Slingerland condensation mechanism. Charge fractionalization results from a Debye-Hückel–type screening cloud formed by the condensed composite particles. Within our general framework, we explore two aspects of symmetry-enriched 3D Abelian topological phases. First, we construct a new fermionic state of matter with time-reversal symmetry and $\Theta \neq \pi$, the fractional topological insulator. Second, we generalize the notion of anyonic symmetry of 2D Abelian topological phases to the *charge-loop excitation symmetry* (Charles) of 3D Abelian topological phases. We show that line twist defects, which realize Charles transformations, exhibit non-Abelian fusion properties.

DOI: 10.1103/PhysRevB.94.115104

I. INTRODUCTION

A. Background and overview: Parton construction and gauge confinement

In models of noninteracting fermions, several topological phases of matter have been found, such as integer quantum Hall states (IQH), Chern insulators, and topological insulators (TI) [1–9]. Owing to the noninteracting nature of the problem, tremendous progress has been made in both theory and experiment. In the presence of weak interactions, these phases can also be analytically understood. If interactions are strong enough such that a perturbative analysis is no longer meaningful, one usually faces a problem in strongly correlated electron physics. While exact solutions are possible in a few specific models, one often constructs approximate effective descriptions of such systems. One such approach is the parton construction approach, also known as the projective construction, or slave-particle approach. It has been widely applied in studies of strongly correlated electron systems such as high-temperature superconductors and fractional quantum Hall states (FQH) [10–32]. Recently, it has also been applied [33–37] to bosonic symmetry-protected topological phases (SPT) as well [38–41].

Generally speaking, in the parton construction we start with a lattice action S that describes a strongly correlated electronic system. In this paper, the electron operator c is meant to represent a generic Grassmann variable that is the only dynamical variable in S. We further write the electron operator c in terms of several parton operators f^i. The Hilbert space for S is equivalently replaced by a projected Hilbert space formed by partons and gauge fields. In practice, there are many different kinds of parton constructions. We focus on one of them, where all partons are fermionic such that an odd number of partons are required to form an electron. Mathematically, the electron operator is formally fractionalized as $c = f^1 f^2 \dots f^{2n+1}$. The electron operator c is a singlet of the SU($2n+1$) gauge group. The largest totally commuting subgroup, or maximal torus, is given by the compact Abelian $[\mathrm{U}(1)]^{2n}$ gauge group which acts with gauge transformations $f^1 \to f^1 e^{i\theta_1}, \dots, f^i \to f^i e^{i\theta_i - i\theta_{i-1}}, \dots, f^{2n+1} \to f^{2n+1} e^{-i\theta_{2n}}$, where $\{\theta_i\}$ ($i = 1,2,\dots,2n$) are arbitrary functions of the lattice sites and a continuous time variable. As such, by applying the 't Hooft gauge projection [42], the lattice action deep in the confined phase is reformulated to describe a system of interacting partons and $2n$ dynamical compact Abelian gauge fields $\{a_\mu^{(i)}\}$.

It should be noted that the gauge-field coupling constants g_i at the lattice scale should be treated as being very strong since the usual lattice kinetic terms (with coefficient $1/g_i^2$) for compact gauge fields are not present in S. From here one can usually proceed further by assuming a mean-field theory of partons where the effects of gauge fluctuations are assumed negligible. As such, a very important feature, the compactness of gauge fields, is totally ignored. A standard perturbative analysis can be applied in order to quantitatively recover the effect of gauge fluctuations at leading order. In some cases, this assumption is legitimate. A typical example is a two-dimensional (2D) system where fermionic partons occupy energy bands with nonzero Chern number at the mean-field level [34]. In this case, a Chern-Simons term is generated and a topological mass gap [43] for the gauge fields is produced,

which suppresses instanton tunneling. However, there is no reason to rule out the possibility that g at low energies flows to strong coupling, such that the compactness of the gauge fields plays a fundamental role in reshaping the nature of the emergent ground states. In such cases, mean-field theories of partons fail to describe the physical states formed by electrons, even at a qualitative level.

Despite the strong coupling nature of the problem, the leading-order effect of gauge fluctuations can still be perturbatively treated by considering the Bose-Einstein condensation of composite particles. In the regime of strong gauge coupling, condensed composites contain magnetic monopoles of the internal compact gauge fields (and possible electric gauge charge as well). Historically, this line of thinking was developed in the context of strongly coupled gauge theories. For example, condensed monopole phases are relevant for studies of (3+1)-dimensional [(3+1)D] compact quantum electrodynamics, the Georgi-Glashow models, and supersymmetric Yang-Mills theory [42,44–54]. For an Abelian gauge theory with a compact U(1) gauge group, the monopole creation operator has been constructed explicitly and gains a nonzero vacuum expectation value as shown in Ref. [52]. Recently, it was further suggested that the behavior of the nontrivial line operators may be used to make the proper distinction between confinement phases of strongly coupled gauge theories [55]. Note that since electric (i.e., gauge) charge excitations are linearly confined during this condensation process, the monopole condensation phase is also called the confinement phase.

Unfortunately, the usual monopole condensation scenario [42,44–54], when applied to the 3D parton construction, will simply confine all partons back into electrons, resulting in a nonfractionalized trivial insulator. In this sense, the parton construction with gauge confinement driven by the usual monopole condensation does not seem to be a good pathway to reach topological states. To save the parton construction approach, we should look for new scenarios of gauge confinement. More precisely, can we have a new kind of condensation that confines partons while still leading to a fractionalized insulator? How can we imagine the existence of fractionalized excitations when partons are confined? If these questions can be solved, a systematic treatment of 3D fermionic fractionalized phases will be established. This is the main goal of this paper, and that this is possible can be gleaned from the success of the 2D Bais-Slingerland condensation mechanism [56]. Indeed, we show that there are new pathways to fractionalization in 3D, now in the *confining regime* of the gauge theory, provided that confinement occurs as the result of condensation of a class of composites made of fermionic partons and monopoles (from different sectors of the gauge group). We will see that this form of *oblique confinement* [42] leads to unexpected phases of matter, particularly states with fractionalized Θ angles and yet compatible with time-reversal invariance. While oblique confinement as a pathway to topological phases has been considered before in the context of bosonic phases of matter [57], here we focus on topological phases of interacting fermions. In addition, we also study several applications. For example, how can we impose symmetry in such a parton construction with gauge confinement? The latter leads to the notion of symmetry-enriched topological phases (SET) in the parton construction approach.

B. Summary of main results

(1) Composite particle theory of fermionic phases. In this paper, we will consider the condensation of "composites" that not only carry magnetic charges, but also contain fermionic partons that are charged under different internal gauge fields [i.e., U(1) × U(1) strongly fluctuating gauge fields in our concrete example $c = f^1 f^2 f^3$] and under the external electromagnetic (EM) field A_μ. One caveat is that, despite the mixture of partons and magnetic monopoles, those condensed composites are *not* dyons. More concretely, they carry either electric charge or magnetic charge in a given gauge group, not both. This fact allows us to make reliable statements and calculations from a *local* theory. All excitations can be organized as a set of *charge-loop composites*, and, as a whole, form a *charge-loop lattice* in which each lattice site corresponds to a deconfined excitation. Especially, partons are confined as usual but some composites constituted by partons and magnetic monopoles of U(1) × U(1) gauge fields may be deconfined and carry fractionalized EM electric charge. Many universal physical properties can be easily determined from the charge-loop lattice, such as the braiding statistics between pointlike excitations and loop excitations, the self-statistics of pointlike excitations, the EM charge of the excitation, and the bulk axion Θ angle [58,59]. We will refer to this approach to constructing 3D fermionic gapped phases as a *composite particle theory*.

In this theory, charge fractionalization is achieved via a Debye-Hückel–type charge-screening cloud formed by the composite condensates. This is analogous to the charge-screening phenomenon in the composite fermion theory of the FQH effect [60–66]. In fact, we prove that the Debye-Hückel–type screening is the unique source of charge fractionalization. In principle, all physical quantities of the resulting phases can be expressed as functions of a set of parameters that characterize composite particle theory. This line of thinking is also analogous to the composite fermion theory of FQH states where the filling fraction is unified in a sequence of discrete numbers, each of which corresponds to a specific *Ansatz* in the composite fermion construction. From this perspective, the composite particle theory may be regarded as an attempt to find a 3D analog of the composite fermion theory of FQH states, with the caveat that we are considering confined phases while in the composite fermion theory, all gauge fields are deconfined.

(2) Fractional topological insulators. Based on the composite particle theory, we will study two symmetry-enriched properties. The first property is the bulk axion angle Θ in the presence of time-reversal symmetry [58,59]. When Θ is nonvanishing, an externally inserted EM monopole with integral magnetic charge M will induce an electric polarization charge $\frac{\Theta}{2\pi}M$, a phenomenon known as the Witten effect [58,59,67]. For free-fermion topological insulators, the Θ angle is $\pi \bmod 2\pi$ with $M \in \mathbb{Z}$ [59]. However, it was theoretically proposed that Θ could be different from π if strong interactions and correlations are taken into account [68–72], leading to the notion of 3D fractional topological insulators (FTI) with deconfined gauge fields. The periodicity of Θ should also be properly modified so as to preserve time-reversal symmetry.

In Ref. [68], FTIs were obtained via parton constructions where the internal gauge fields are in the Coulomb phase (photons are gapless). Therefore, a gapless channel, despite of its electric neutrality, can in principle adiabatically connect the FTIs to a fractionalized state with vanishing axion angle. In Ref. [71], bosonic FTIs were obtained via parton constructions where the mean-field Hamiltonian of partons explicitly breaks SU(2) gauge group down to $\mathbb{Z}_2$ discrete gauge group. As a result, the unbroken discrete gauge group leads to bulk topological order and deconfined fractionalized excitations. The gauge fluctuations in both Refs. [68,71] are perturbatively weak. In this work, we explore the possibility of realizing FTIs via the condensation of composites (introduced above) when gauge fluctuations are sufficiently strong and gauge confinement occurs.

In Refs. [68,71], each parton is assumed to carry a fractional EM electric charge such that a fractionalized Θ angle should be expected (by simply noting that the coefficient of $F \wedge F$ has unit of e^2). This is not the case in our work. We show that even if partons carry integral EM electric charge (i.e., both f^1 and f^2 carry $+1$ electric charge and f^3 carries -1 electric charge, see Sec. II A for more details), a fractionalized Θ and gapped bulk can also be achieved as long as a proper composite condensation is considered and partons occupy nontrivial topological insulator bands. This feature is unique in the parton construction with gauge confinement.

In the FTI state constructed in this work (Secs. III B and III C), we show that the EM electric charge of deconfined excitations is fractionalized at $\frac{1}{3}$. This is consistent to the claim by Swingle *et al.* [71] that an FTI necessarily has a fractionalized bulk. Indeed, the fractionalization nature of the FTI state in this work can be traced back to the presence of $\mathbb{Z}_2 \times \mathbb{Z}_6$ topological order (see Sec. III C for more details). The latter arises from the deconfined discrete subgroup of the confined SU(3) gauge group.

(3) Charge-loop excitation symmetry and extrinsic twist defects. Noting that the set of all excitations forms a charge-loop lattice, the second symmetry-enriched property is the concept of "charge-loop excitation symmetry," abbreviated as Charles (see Definition 5). Charles can be viewed as a hidden symmetry of (3+1)D topological quantum field theories. Meanwhile, Charles has a geometric interpretation as a point-group symmetry of the charge-loop lattice that preserves physical properties of the excitations. The study of Charles is motivated by the theory of anyonic symmetry [73–84] and its relation to extrinsic twist defects of 2D Abelian topological phases. We expect that 3D Abelian topological phases where charge-loop composite excitations are allowed may host even more exotic physics if extrinsic defects are considered.

Physically, extrinsic defects (which may come in the form of vortices or disclinations, for example) are semiclassical objects that are externally imposed into a 2D topological phase. An extrinsic *twist* defect is one which may be associated with an element of an anyonic symmetry group that acts to permute the set of anyons. The inclusion of such defects enriches the tensor category theory of the Abelian parent topological phase. Indeed, this line of thinking has attracted a lot of attention since extrinsic twist defects can bind non-Abelian objects even though all of excitations of the parent topological phase without defects are Abelian [79–84]. A typical example is found in some lattice systems exhibiting $\mathbb{Z}_N$ topological order that contain, for example, the $\mathbb{Z}_N$ charge and flux anyons e and m [79,84]. In these cases, the anyonic symmetry is intertwined with a lattice translation symmetry such that a dislocation defect acts to exchange the e particle type with the m particle type when they orbit around the defect. This implies that the defect harbors a rich internal (non-Abelian) structure so that it can convert between the anyon types. In this work, we propose Charles as a 3D version of anyonic symmetry in 2D. In analogy to 2D, each extrinsic defect in 3D is also associated with a Charles group element. We also study defect species and some defect fusion properties (see Fig. 7).

The remainder of the paper is organized as follows. Section II is devoted to a general discussion of the parton construction and composite condensation. In Sec. III, FTIs are constructed from a composite condensation phase where all of the partons occupy topological insulator bands. A concrete example with time-reversal symmetry and fractional $\Theta = \frac{\pi}{9} \bmod \frac{2}{9}\pi$ is shown (see Fig. 5, Sec. III). As a comparison, we also show a parton construction in the Coulomb (gapless photon) phase using a perturbative approach, which leads to $\Theta = \pi \bmod 2\pi$ and two gapless neutral modes in the bulk. In Sec. IV, the charge-loop excitation symmetry (Charles) of the charge-loop excitations, and its relation to 3D extrinsic defects, is studied. Section V is devoted to the conclusion and future directions. Many key notations, mathematical formulas, and terminologies are introduced in Sec. II, which provides the preliminaries for the subsequent parts. Several technical details can be found in the Appendixes. In Appendix A, several notations and abbreviations are collected.

II. COMPOSITE PARTICLE THEORY IN THREE DIMENSIONS: A GENERAL DISCUSSION

A. Compact U(1) × U(1) × U(1) gauge symmetry of composites

In the simplest fermionic parton construction, the electron operator is decomposed into three fermionic partons: $c = f^1 f^2 f^3$ (Fig. 1), where both f^1 and f^2 carry unit EM charge e while f^3 carries $-e$. As a result, the electron carries e. In a 3D mean-field theory where the partons are deconfined, we consider that all fermionic partons have a gapped spectrum

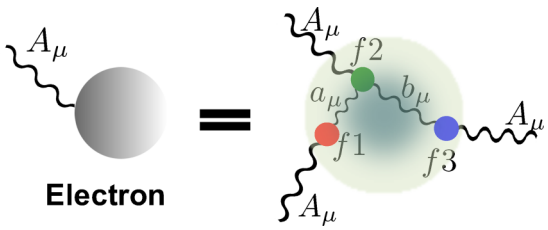

FIG. 1. Parton construction of electron operators in this work. The wavy lines denote interactions mediated by gauge bosons. A_μ is the external nondynamical EM (electromagnetic) field, serving as a probe of the electromagnetic response of the system. a_μ and b_μ are two dynamical, compact U(1) gauge fields, belonging to the $U(1)_a$ and $U(1)_b$ gauge groups, respectively. The partons f^1 and f^2 carry 1 and -1 gauge charges of the $U(1)_a$ gauge group, respectively. The partons f^3 and f^2 carry 1 and -1 gauge charges of the $U(1)_b$ gauge group, respectively. The EM electric charges carried by the partons f^1, f^2, f^3 are e, e, $-e$, respectively.

and form either a trivial band insulator ($\theta = 0$) or a strong topological insulator ($\theta = \pi$) simultaneously, where θ denotes the axion angle of the partons [58,59]. To avoid confusion, we will use the capital letter Θ to denote the axion angle of the electron, which will be calculated in detail in Sec. III. The internal gauge group is SU(3) whose maximal torus (maximal commuting subgroup) $\mathrm{U}(1)_a \times \mathrm{U}(1)_b$ is sufficient to capture the confinement phase properties due to the 't Hooft gauge projection [42]. Here, both U(1) factors are compact gauge groups that support magnetic monopoles [42]. $\mathrm{U}(1)_a$ corresponds to the gauge field a_μ that glues f^1 and f^2 together, while $\mathrm{U}(1)_b$ corresponds to the gauge field b_μ that glues f^2 and f^3 together (Fig. 1). Adding the EM gauge group with gauge field A_μ, the total gauge group is given by $\mathrm{U}(1)_a \times \mathrm{U}(1)_b \times \mathrm{U}(1)_{\mathrm{EM}}$. It should be noted that A_μ is a nondynamical (i.e., background) gauge field, which is useful for diagnosing the EM linear response properties of the resulting phases. For the same reason, we consider monopole configurations of A_μ (with magnetic charge M) as externally imposed background configurations.

Alternatively, one may also define the following three gauge fields:

$$A_\mu^{f1} = a_\mu + A_\mu, \quad A_\mu^{f2} = -a_\mu - b_\mu + A_\mu, \quad A_\mu^{f3} = b_\mu - A_\mu,$$

where A^{fi} is the gauge field that only couples to f^i ($i = 1,2,3$). The relation between the two sets of gauge fields can be expressed in matrix form

$$\begin{pmatrix} A_\mu \\ a_\mu \\ b_\mu \end{pmatrix} = \begin{pmatrix} 1 & 1 & 1 \\ 0 & -1 & -1 \\ 1 & 1 & 2 \end{pmatrix} \begin{pmatrix} A_\mu^{f1} \\ A_\mu^{f2} \\ A_\mu^{f3} \end{pmatrix}, \tag{1}$$

where the matrix is integer valued and invertible, i.e., belongs to the $\mathbb{GL}(3,\mathbb{Z})$ group. We now turn to the description of generic composite particles, which are labeled by a set of electric charges and magnetic charges. We use $N_{a,b}$ to denote the electric charge of the $\mathrm{U}(1)_{a,b}$ gauge group and $N_m^{a,b}$ to denote the magnetic charge of that same gauge group. We use N_A and M to denote the bare electric and magnetic charges in the EM gauge group, and N^{fi} and N_m^{fi} to denote the electric and magnetic charges of the $\mathrm{U}(1)_{fi}$ gauge groups.

Due to Eq. (1), the magnetic charges transform as

$$\begin{aligned} N_m^{f1} &= N_m^a + M, \\ N_m^{f2} &= -N_m^a - N_m^b + M, \\ N_m^{f3} &= N_m^b - M, \end{aligned}$$

and electric charges transform as

$$\begin{aligned} N_A &= N^{f1} + N^{f2} - N^{f3}, \\ N_a &= N^{f1} - N^{f2}, \\ N_b &= N^{f3} - N^{f2}. \end{aligned}$$

For convenience, we can easily derive the following useful formulas:

$$\begin{aligned} M &= N_m^{f1} + N_m^{f2} + N_m^{f3}, \\ N_m^a &= -N_m^{f2} - N_m^{f3}, \\ N_m^b &= N_m^{f1} + N_m^{f2} + 2N_m^{f3}. \end{aligned}$$

To summarize, a composite particle can be uniquely labeled by six numbers (three electric charges and three magnetic charges). The above relations can be recast in matrix form

$$\begin{pmatrix} N_A \\ N_a \\ N_b \end{pmatrix} = \begin{pmatrix} 1 & 1 & -1 \\ 1 & -1 & 0 \\ 0 & -1 & 1 \end{pmatrix} \begin{pmatrix} N^{f1} \\ N^{f2} \\ N^{f3} \end{pmatrix}, \tag{2}$$

$$\begin{pmatrix} M \\ N_m^a \\ N_m^b \end{pmatrix} = \begin{pmatrix} 1 & 1 & 1 \\ 0 & -1 & -1 \\ 1 & 1 & 2 \end{pmatrix} \begin{pmatrix} N_m^{f1} \\ N_m^{f2} \\ N_m^{f3} \end{pmatrix}, \tag{3}$$

where the two matrices belong to the $\mathbb{GL}(3,\mathbb{Z})$ group. All magnetic charges take values in an integral domain, i.e., M, N_m^a, N_m^b, $N_m^{fi} \in \mathbb{Z}$, where $i = 1,2,3$. However, we will soon see that this integral domain will be potentially restricted to a smaller domain if we only consider the deconfined *excitations* in the presence of a composite condensate. We will introduce the notion of excitations in Sec. II D.

By the bare electric charge, we mean that N_A is a naive count of the EM electric charge. In Sec. II D, it will be shown that composite condensates will partially screen the charge, leading to a *net* EM electric charge Q to be defined in Eq. (28). The electric charges N^{fi} ($i = 1,2,3$) are related to the number of attached fermions via the Witten effect formula

$$N^{fi} = n^{fi} + \frac{\theta}{2\pi} N_m^{fi}, \quad \text{with} \quad n^{fi} \in \mathbb{Z}. \tag{4}$$

The integer n^{fi} counts the total number of fermions f^i in the composite, and θ is determined by the $\mathbb{Z}_2$ index of a 3D time-reversal-invariant topological insulator. If $\theta = 0$, the partons occupy a trivial band structure; if $\theta = \pi$, the partons occupy a nontrivial topological insulator band structure. The defining domains of $N^{f1,f2,f3}, N_a, N_b, N_A$ can be either integer or potentially half-integer, depending on θ.

B. A local field-theoretic description of condensed composites

Since there are two internal gauge fields with strong gauge fluctuations, we can consider two linearly independent Bose condensates denoted by φ_1 and φ_2, as shown in Fig. 2. Both condensates should contain magnetic monopoles of the internal gauge fields but be neutral under both the $\mathrm{U}(1)_a$ and $\mathrm{U}(1)_b$ gauge groups, i.e., $N_a = 0$, $N_b = 0$. Since the EM gauge field is treated as a background gauge field for the purpose of the EM response, the condensates should not carry M. Otherwise, the EM gauge field must be strongly fluctuating, which is not our working assumption. In summary, the electric and magnetic charges of φ_1 and φ_2 can be completely determined by six parameters (q,u,v,q',u',v') in Table I. Since the condensates are not dyonic in each gauge group the order parameters $\langle\varphi_1\rangle$ and $\langle\varphi_2\rangle$ are local to each other and can be described by an effective local quantum field theory. More concretely, we may start with a phenomenological Ginzburg-Landau–type action in 4D Euclidean space-time:

$$S_{\mathrm{GL}} = \int d^4x \sum_I^2 (|\hat{D}_\mu \varphi_I|^2 + \mu^2 |\varphi_I|^2 + \lambda |\varphi_I|^4) + S_M, \tag{5}$$

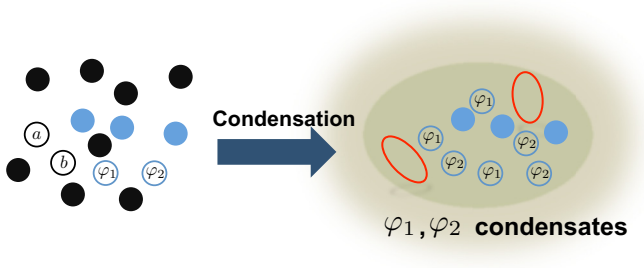

FIG. 2. Schematic representation of composite particle condensation. Before condensation, the system is an electromagnetic plasma of composites in the $U(1)_{EM} \times U(1)_a \times U(1)_b$ gauge group. There are many composite particles (denoted by solid circles) including φ_1 and φ_2. There are also two gapless photons (denoted by a and b in the figure), indicating that the phase before condensation is a gapless Coulomb phase for both internal dynamical gauge fields. After condensing φ_1 and φ_2, the system enters a gapped phase in the absence of photons. All composites (denoted by black solid circles on the left) that have nonzero mutual statistics with both φ_1 and φ_2 are confined. Otherwise, those composites that have trivial (zero) mutual statistics with both condensates survive as excitations (denoted by blue solid circles) of the gapped phase. The red loops on the right represent loop excitations due to the two condensates.

where the Ginzburg-Landau parameter λ is positive. $\hat{D}_\mu$ is the covariant derivative defined by

$$\hat{D}_\mu \equiv \partial_\mu + iN_A A_\mu + iN_m^a \tilde{a}_\mu + iN_m^b \tilde{b}_\mu. \tag{6}$$

Here, N_A, N_m^a, N_m^b are two sets of electric/magnetic charges of φ_1 and φ_2, which can be found in Table I. The one-form gauge fields $\tilde{a}_\mu$ and $\tilde{b}_\mu$ serve as the magnetic dual of the gauge fields a_μ and b_μ, respectively. For example, $\tilde{a}_\mu$ is introduced such that its gauge charge is carried by magnetic monopoles of the $U(1)_a$ gauge group. Meanwhile, the magnetic flux of $\tilde{a}_\mu$ gives the electric field $\mathbf{E}^a$, namely, $\mathbf{E}^a = \nabla \times \tilde{\mathbf{a}}$. $\tilde{b}_\mu$ can be understood analogously to $\tilde{a}_\mu$. S_M includes the Maxwell terms: $S_M = \int d^4x (\frac{1}{4}\tilde{f}^a_{\mu\nu}\tilde{f}^a_{\mu\nu} + \frac{1}{4}\tilde{f}^b_{\mu\nu}\tilde{f}^b_{\mu\nu})$. In the condensed phase where the mass parameter $\mu^2 < 0$, nonzero expectation values $\langle\varphi_I\rangle \neq 0$ develop. Here, $\tilde{f}^{a,b}_{\mu\nu}$ are the field strength tensors of $\tilde{a}_\mu$ and $\tilde{b}_\mu$. One advantage to using dual gauge fields is that the problem of strong gauge fluctuations ($g_a \gg 1$, $g_b \gg 1$) of the a_μ and b_μ gauge fields is transformed into the problem of weak gauge fluctuations of the dual gauge fields $\tilde{a}_\mu$ and $\tilde{b}_\mu$ by noting that the coupling constants between magnetic charges and dual gauge fields is the inverse of the original coupling constants, i.e., $1/g_{a,b}$.

It is noteworthy that the six numbers (u,v,u',v',q,q') describing the condensates are not completely free since the following three conditions should be satisfied:

(1) φ_1 and φ_2 are bosonic;
(2) φ_1 and φ_2 are allowed to condense simultaneously;
(3) φ_1 and φ_2 are linearly independent,

such that the composite condensates φ_1 and φ_2 are physically viable. In more detail, according to the domains of definition of every charge (e.g., all magnetic charges are integer valued, all n^{fi} are integer valued), we can deduce the domains of the six numbers (see Table I):

$$u, v, u', v', q - \frac{\theta}{2\pi}u, \quad q + \frac{\theta}{2\pi}(u+v), \quad q - \frac{\theta}{2\pi}v \in \mathbb{Z}, \tag{7}$$

$$q' - \frac{\theta}{2\pi}u', \quad q' + \frac{\theta}{2\pi}(u'+v'), \quad q' - \frac{\theta}{2\pi}v' \in \mathbb{Z}. \tag{8}$$

Since only bosonic particles can undergo Bose condensation, one should carefully check the self-statistics of φ_1 and φ_2. Furthermore, the mutual statistics between φ_1 and φ_2 must be zero so that they are allowed to condense simultaneously.

Let us first consider the latter. The trivial mutual statistics between two composites (with and without prime) is given by the following equation:

$$\sum_i^3 \left(N_m^{fi} n^{fi'} - N_m^{fi'} n^{fi}\right) = 0 \tag{9}$$

TABLE I. The electric charges and magnetic charges of composite condensates φ_1 and φ_2 are determined by parameters (u,v,u',v',q,q',θ). The charges are shown for both the $U(1)_a \times U(1)_b \times U(1)_{EM}$ gauge group labels and the $U(1)_{f1} \times U(1)_{f2} \times U(1)_{f3}$ gauge group labels, both of which are used interchangeably in the main text. The two sets of parameters are related via Eqs. (2) and (3). The value of $\theta = 0, \pi$ is determined by the band-structure topology of the partons. Given θ, the other six parameters are constrained by several conditions listed in Eqs. (7), (8), (12), and (13). A concrete example of composite condensates that generates a fractional topological insulators (FTI) with $\Theta = \frac{\pi}{9}$ discussed in Sec. III B is also shown. For this case, we see that φ_1 is a bosonic bound state of two a_μ magnetic monopoles, two b_μ magnetic monopoles, one f^1 parton, four f^2 partons, and one f^3 parton, while φ_2 is a bosonic bound state of four a_μ magnetic monopoles, ten b_μ magnetic monopoles, nine f^2 partons, and three holelike f^3 partons. We may call the partons themselves as the simplest composites although literally they are not composites. Also, the electron is just a collection of one f^1, one f^2, and one f^3.

	$U(1)_a \times U(1)_b \times U(1)_{EM}$						$U(1)_{f1} \times U(1)_{f2} \times U(1)_{f3}$								
Composite particles	N_a	N_b	N_A	N_m^a	N_m^b	M	N^{f1}	N^{f2}	N^{f3}	N_m^{f1}	N_m^{f2}	N_m^{f3}	n^{f1}	n^{f2}	n^{f3}
φ_1	0	0	q	u	v	0	q	q	q	u	$-u-v$	v	$q - \frac{\theta}{2\pi}u$	$q + \frac{\theta}{2\pi}(u+v)$	$q - \frac{\theta}{2\pi}v$
φ_2	0	0	q'	u'	v'	0	q'	q'	q'	u'	$-u'-v'$	v'	$q' - \frac{\theta}{2\pi}u'$	$q' + \frac{\theta}{2\pi}(u'+v')$	$q' - \frac{\theta}{2\pi}v'$
φ_1 of FTI in Sec. III B	0	0	2	2	2	0	2	2	2	2	−4	2	1	4	1
φ_2 of FTI in Sec. III B	0	0	2	4	10	0	2	2	2	4	−14	10	0	9	−3
Parton f^1	1	0	1	0	0	0	1	0	0	0	0	0	1	0	0
Parton f^2	−1	−1	1	0	0	0	0	1	0	0	0	0	0	1	0
Parton f^3	0	1	−1	0	0	0	0	0	1	0	0	0	0	0	1
Electron	0	0	1	0	0	0	1	1	1	0	0	0	1	1	1

or, equivalently, $\sum_i^3 (N_m^{fi} N^{fi'} - N_m^{fi'} N^{fi}) = 0$. If this equation is satisfied, then the two composites can condense simultaneously. Furthermore, condensation of one of the composites will lead to deconfined particles (an excitation spectrum) having electric and magnetic charges are determined by this equation. If the equation is not satisfied, the condensation of one of the composites will confine the other [85,86]. Inserting the electric and magnetic charges of φ_1,φ_2 into the equation, it turns out that φ_1 and φ_2 always satisfy the condition of trivial mutual statistics.

Next, we need to further check the self-statistics of φ_1 and φ_2. For a generic composite, the self-statistics phase $e^{i\pi\Gamma}$ is determined by the following integer:

$$\Gamma = \sum_i^3 \left(N_m^{fi} n^{fi} + n^{fi}\right), \tag{10}$$

where the second term n^{fi} counts the number of fermionic partons inside the composite. The first term $N_m^{fi} n^{fi}$ arises from the angular momentum of the relative motion between the electric charge and magnetic charge. Note that the polarization charge "$\frac{\theta}{2\pi} N_m^{fi}$" due to the Witten effect in Eq. (4) does not enter the statistics. A field-theoretic understanding of this phenomenon can be found in Ref. [87]. For later convenience, we may express Eq. (10) in terms of the $\mathrm{U}(1)_{\mathrm{EM}} \times \mathrm{U}(1)_a \times \mathrm{U}(1)_b$ gauge groups:

$$\begin{aligned}\Gamma = {} & N_m^a (n^{f1} - n^{f2}) + N_m^b (n^{f3} - n^{f2}) \\ & + (M+1)(n^{f1} + n^{f2} - n^{f3}),\end{aligned} \tag{11}$$

where we have added even integers during the derivation as only the value of Γ mod 2 is meaningful. If Γ is even, the composite is bosonic; otherwise, it is fermionic. After inserting the values of the electric and magnetic charges of φ_1 and φ_2 into Γ, we may obtain the Γ formulas of both φ_1 and φ_2 [denoted as $\Gamma(\varphi_1),\Gamma(\varphi_2)$] as functions of u,v,u',v',q,q' (see Appendix B 1). The requirement that both φ_1 and φ_2 are bosonic leads to the following constraints on u,v,u',v',q,q':

$$\Gamma(\varphi_1) \in \mathbb{Z}_{\mathrm{even}}, \quad \Gamma(\varphi_2) \in \mathbb{Z}_{\mathrm{even}}. \tag{12}$$

So far, we have deduced several constraints on the six numbers: Eqs. (7), (8), and (12), but there is one more constraint, i.e., Eq. (13), which enforces that φ_1 and φ_2 are linearly independent. It is possible that one of the composites consists of several copies of the other composite, in which case there is actually only one condensate. To avoid this situation, the following condition should be strictly imposed:

$$uv' - u'v \neq 0. \tag{13}$$

A physical understanding of this condition will be presented in Sec. II C. For convenience, we introduce the following notation:

$$K = \begin{pmatrix} u & v \\ u' & v' \end{pmatrix}, \quad \mathbf{N}_m = \begin{pmatrix} N_m^a \\ N_m^b \end{pmatrix}, \quad \mathbf{q} = \begin{pmatrix} q \\ q' \end{pmatrix}, \tag{14}$$

$$\Phi_e = \begin{pmatrix} \Phi_e^a \\ \Phi_e^b \end{pmatrix}, \quad \mathbf{N}_e = \begin{pmatrix} N_a \\ N_b \end{pmatrix}. \tag{15}$$

Then, the matrix K is invertible, namely, its determinant should be nonzero, as given by Eq. (13). In summary, the conditions (7), (8), (12), and (13) should be imposed on the six integers $u,v,q;u',v',q'$ such that the two condensates satisfy conditions 1, 2, and 3.

C. Generalized flux quantization and loop excitations

In order to gain a better physical understanding of the condition (13), we need to carefully study the "generalized flux quantization" induced by the two condensates φ_1 and φ_2 whose electric and magnetic charges are listed in Table I. In a usual type-II superconductor, we know that the EM magnetic flux denoted by Φ_M^A is screened and quantized according to $2\Phi_M^A/2\pi = \Phi_M^A/\pi \in \mathbb{Z}$ since the Cooper pair condensate carries $2e$ EM electric charge. In our case, the two condensates φ_1 and φ_2 carry not only EM electric charges but also magnetic charges of the a and b gauge groups as shown in Table I. As a result, we have the following generalized flux quantization conditions:

$$q\Phi_M^A + u\Phi_e^a + v\Phi_e^b = 2\pi\ell, \tag{16}$$

$$q'\Phi_M^A + u'\Phi_e^a + v'\Phi_e^b = 2\pi\ell', \tag{17}$$

where Φ_M^A is the EM magnetic flux piercing a spatial loop $\mathcal{S}^1$. Φ_e^a and Φ_e^b are the a- and b-electric fluxes piercing $\mathcal{S}^1$, respectively. Here, instead of magnetic fluxes, electric fluxes of the $\mathrm{U}(1)_a \times \mathrm{U}(1)_b$ gauge group are involved since the condensates carry magnetic charges rather than electric charges of the $\mathrm{U}(1)_a \times \mathrm{U}(1)_b$ gauge group. $\ell,\ell' \in \mathbb{Z}$ label the winding numbers of the mapping $\mathcal{S}^1 \to \mathrm{U}(1)$ of the condensate order parameters φ_1,φ_2.

In contrast with fluxes of the internal gauge groups, arbitrary values of Φ_M^A are allowed to be inserted. In other words, A_μ itself is not Higgsed, and the EM electric charge of the electrons is a well-defined quantum number. This implies that the two condensates must provide a new charge screening mechanism such that the net EM electric charge of each condensate is zero, although both condensates carry a nonzero bare EM electric charge ($N_A = q,q'$). This screening effect can lead to fractionalization of the charge of excitations, even in the absence of an external EM magnetic charge. We will postpone a discussion of this issue until Sec. II D.

Since A_μ is an external nondynamical field, we may temporarily turn it off in Eqs. (16) and (17) to find

$$u\Phi_e^a + v\Phi_e^b = 2\pi\ell, \quad u'\Phi_e^a + v'\Phi_e^b = 2\pi\ell'. \tag{18}$$

A generic solution of Eq. (18) is given by

$$\Phi_e^a = 2\pi\frac{\ell v' - \ell' v}{\mathrm{Det}K}, \quad \Phi_e^b = 2\pi\frac{\ell' u - \ell u'}{\mathrm{Det}K}. \tag{19}$$

Here, $u,v,u',v' \in \mathbb{Z}$ satisfy the condition (13). By noting that $\ell v' - \ell' v$ is divisible by the greatest common divisor $\mathrm{GCD}(v,v')$ and $\ell' u - \ell u'$ is divisible by the greatest common divisor $\mathrm{GCD}(u,u')$, one can use Bézout's lemma (see Appendix B 2) to obtain the minimal quantized electric fluxes:

$$\left(\Phi_e^a\right)_{\min} = 2\pi\left|\frac{\mathrm{GCD}(v,v')}{\mathrm{Det}K}\right|, \quad \left(\Phi_e^b\right)_{\min} = 2\pi\left|\frac{\mathrm{GCD}(u,u')}{\mathrm{Det}K}\right|. \tag{20}$$

Since $|uv' - u'v|$ is divisible by both $\mathrm{GCD}(v,v')$ and $\mathrm{GCD}(u,u')$, we have the following two useful inequalities:

$$|uv' - u'v| \geqslant |\mathrm{GCD}(u,u')|, \quad |uv' - u'v| \geqslant |\mathrm{GCD}(v,v')|. \tag{21}$$

Based on Bézout's lemma, we can easily prove the following theorem. The proof is shown in Appendix B 2.

Theorem 1. $(\Phi_e^a)_{\min} = 2\pi$ and $(\Phi_e^b)_{\min} = 2\pi$ if and only if $|uv' - u'v| = 1$.

The above theorem leads to the following criterion for loop/flux excitations:

Criterion 1 (Criterion for loop excitations). If $|\mathrm{Det}K| = 1$, the bulk has no deconfined discrete gauge fluxes (therefore, no detectable loop excitations). If $|\mathrm{Det}K| > 1$, the bulk has deconfined discrete gauge fluxes (therefore, detectable loop excitations with minimal flux strength smaller than 2π).

The solutions (Φ_e^a, Φ_e^b) in Eq. (19) can be recast in the following form:

$$\Phi_e = 2\pi K^{-1}\mathbf{L}, \tag{22}$$

where the integer vector $\mathbf{L} = (\ell, \ell')^T$. Thus, we may define a 2D loop lattice generated by a dimensionless integer vector $\mathbf{L}$:

Definition 1 (Loop lattice). A loop lattice is a 2D square lattice where each site corresponds to a loop excitation labeled by $\mathbf{L} = (\ell, \ell')^T$. The corresponding electric flux strength Φ_e of each site is determined by Eq. (22).

D. Point-particle excitations and charge fractionalization

In addition to loop excitations, we also have point-particle excitations:

Definition 2 (Excitation and charge lattice). Excitations are defined as deconfined particles that have trivial mutual statistics with both condensates. All excitations form a 4D charge lattice which is a sublattice of the original 6D lattice. Unless otherwise specified, excitations always refer to point-particle excitations.

By definition, all excitations have trivial mutual statistics with respect to the condensates. In other words, Eq. (9) holds between any excitation and φ_1, and also holds between any excitation and φ_2. By explicitly using the parameters of φ_1 and φ_2 in Table I, the electric and magnetic charges of excitations are constrained by the following two equations:

$$qM = uN_a + vN_b, \quad q'M = u'N_a + v'N_b. \tag{23}$$

Therefore, a generic particle that has six independent charges $(N_A, N_a, N_b, M, N_m^a, N_m^b)$ is now completely determined by four of them (N_A, M, N_m^a, N_m^b) if the particle is a deconfined excitation in the condensed phase. Keeping Eq. (13) in mind, N_a and N_b are fully determined by M: $N_a = \frac{qv'-q'v}{\mathrm{Det}K}M$, $N_b = \frac{q'u-qu'}{\mathrm{Det}K}M$ which can be written as

$$\mathbf{N}_e = MK^{-1}\mathbf{q} \tag{24}$$

by using the notation in Eqs. (14) and (15).

As mentioned in Sec. II, the EM electric charge of a particle N_A is called the "bare" charge, which suggests that it will be partially screened due to the condensates. In order to clearly see the screening, we turn on the external EM field A_μ to probe the EM response and consider a spatial loop C. The total Aharonov-Bohm phase accumulated by an adiabatically moving test particle is given by (see Fig. 3)

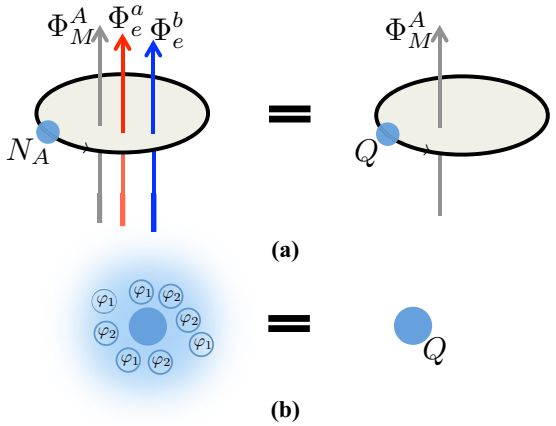

FIG. 3. Schematic representation of the charge-screening mechanism. Consider a composite particle carrying N_A units of the EM (A_μ) electric charge [i.e., U(1) symmetry charge], N_m^a units of magnetic charge of the a_μ field, and N_m^b units of magnetic charge of the b_μ gauge field. Due to the condensates, N_A is partially screened such that the net EM electric charge Q is given by Eq. (28), which is different from N_A. In (a) the physics of Aharonov-Bohm effect in Eq. (25) is illustrated. An excitation (denoted by the blue ball) adiabatically moves along a closed trajectory and feels the EM magnetic flux Φ_M^A, the electric flux Φ_e^a of the a_μ gauge field, and the electric flux of the b_μ gauge field. In (b), condensed particles φ_1 and φ_2 form a Debye-Hückel–type charge cloud around an excitation, providing the screening charge Q_{Debye} in Eq. (29).

Aharonov-Bohm phase

$$= \exp\left\{iN_A\Phi_M^A + iM\Phi_E^A + iN^a\Phi_m^a + iN^b\Phi_m^b + iN_m^a\Phi_e^a + iN_m^b\Phi_e^b\right\}, \tag{25}$$

where Φ_E^A is EM electric flux piercing C, Φ_m^a and Φ_m^b are the a- and b-magnetic fluxes, respectively. However, Eqs. (16) and (17) indicate that Φ_e^a and Φ_e^b depend linearly on the external EM magnetic flux Φ_M^A. Solving Eqs. (16) and (17) leads to

$$\Phi_e^a = 2\pi\frac{kv'-k'v}{\mathrm{Det}K} - \Phi_M^A\frac{qv'-q'v}{\mathrm{Det}K}, \tag{26}$$

$$\Phi_e^b = 2\pi\frac{k'u-ku'}{\mathrm{Det}K} - \Phi_M^A\frac{q'u-qu'}{\mathrm{Det}K}. \tag{27}$$

The terms that depend linearly on Φ_M^A correct the saddle-point solutions in Eq. (19).

Taking Eqs. (26) and (27) into account, the contribution to the Aharonov-Bohm phase due to the external EM gauge field can be isolated. Equation (25) can be recast into $e^{iQ\Phi_M^A+\cdots}$, where the ellipsis denotes the remaining terms that do not contain the factor Φ_M^A, and, Q is the *net EM electric charge*:

$$Q = N_A - Q_{\mathrm{Debye}}, \tag{28}$$

where

$$Q_{\mathrm{Debye}} = N_m^a\frac{qv'-q'v}{\mathrm{Det}K} + N_m^b\frac{q'u-qu'}{\mathrm{Det}K} = \mathbf{N}_m^T K^{-1}\mathbf{q} \tag{29}$$

denotes the charge carried by the Debye-Hückel–type screening cloud (see Fig. 3). The matrix K, vector $\mathbf{N}_m$, and the

vector $\mathbf{q}$ are defined in Eq. (15). Concerning the screening charge, there are two interesting limits. First, the total EM electric charge of each condensate is zero, i.e., $Q = 0$ for both condensates φ_1 and φ_2 (see Table I). For example, we have $Q_{\text{Debye}} = q$ for φ_1, which completely screens its bare EM electric charge $N_A = q$. Second, let us consider an intrinsic excitation whose bare EM electric charge vanishes, $N_A = 0$. Its net EM electric charge Q is nonzero and completely given by that of the Debye screening cloud: $Q = -Q_{\text{Debye}} = -\mathbf{N}_m^T K^{-1}\mathbf{q}$.

In fact, charge fractionalization in Abelian FQH states can also be understood via the above Aharonov-Bohm thought experiment. As an example, let us derive the fractionalization of charge in the $\nu = \frac{1}{3}$ Laughlin state. The effective field theory is described by the following Lagrangian:

$$\mathcal{L} = \frac{3}{4\pi} a_\mu \partial_\nu a_\lambda \epsilon^{\mu\nu\lambda} + \frac{1}{2\pi} A_\mu \partial_\nu a_\lambda \epsilon^{\mu\nu\lambda}. \tag{30}$$

Here, the gauge field a_μ is a dual description of the electron current J_μ: $J_\mu = \frac{1}{2\pi}\partial_\nu a_\lambda \epsilon^{\mu\nu\lambda}$. The second term in the Lagrangian $\mathcal{L}$ means that each electron carries one unit of electric charge. Excitations in FQH states are labeled by gauge charges of the a_μ gauge group since they minimally couple to a_μ. In this sense, let us consider the Aharonov-Bohm experiment for an excitation that carries one unit of gauge charge of a_μ. The Aharonov-Bohm phase is given by $e^{i\Phi_a}$ where Φ_a is the a_μ magnetic flux felt by the excitation. In the hydrodynamical field theory $\mathcal{L}$, $\frac{1}{2\pi}\Phi_a$ corresponds to the electron density. By studying the equation of motion of a_μ in $\mathcal{L}$, we obtain $\Phi_A = 3\Phi_a$. Physically, this identity means that each electron effectively corresponds to three units of magnetic flux of the background EM field, which is nothing but the definition of filling fraction $\nu = \frac{1}{3}$. Thus, the Aharonov-Bohm phase accumulated by the excitation is identical to $e^{i\Phi_a} = e^{i\frac{1}{3}\Phi_A}$. The coefficient $\frac{1}{3}$ indicates that the excitation in the presence of A_μ behaves as an electrically charged particle with $\frac{1}{3}$ charge.

Let us come back to our 3D system. We introduce the following two equivalent criteria for charge fractionalization:

Criterion 2 (Criterion for charge fractionalization). Charge fractionalization exists if excitations with zero M and fractionalized Q exist.

Criterion 3 (Criterion for charge fractionalization). Equivalently, charge fractionalization exists if the EM magnetic charge M of excitations is quantized in units of an integer $w > 1$, i.e., $M = 0, \pm w, \pm 2w, \ldots$.

In Appendix B 3, the equivalence of the above two criteria is explained by using the well-known Dirac-Zwanziger-Schwinger quantization condition. The requirement of $M = 0$ in Criterion 2 can be understood as follows. Typically, in the presence of M, excitations can potentially carry a fractionalized Q due to the Witten effect. However, this does not mean our 3D quantum system is fractionalized. The topological insulator (TI) is a typical example. If a single EM monopole ($M = 1$) is inserted into the bulk, there is a half-charge cloud surrounding the monopole [59,67]. However, since the TI can be realized in a noninteracting band insulator, we do not consider it to be fractionalized. In order to highlight the set of excitations with $M = 0$, we introduce the notion of intrinsic excitations and intrinsic charge lattice.

Definition 3 (Intrinsic excitations and intrinsic charge lattice). Intrinsic excitations are excitations with zero EM magnetic charge, i.e., $M = 0$; the intrinsic charge lattice is a special 3D charge lattice with zero EM magnetic charge, i.e., $M = 0$.

One can verify that Q_{Debye} in Eq. (28) is the *unique* source of charge fractionalization. In other words, N_A in Eq. (28) is always integer valued when $M = 0$ (see Appendix B 4 for details); charge fractionalization exists if and only if Q_{Debye} is fractional when $M = 0$.

Finally, we show that the Debye charge cloud Q_{Debye} in Eq. (29) can also be understood in a more formal way, i.e., from a topological BF field theory. Without loss of generality, we consider the London limit (i.e., deep in the confined phase) such that the amplitude fluctuations of $|\varphi_I|$ are negligible. In this limit, we may dualize S_{GL} in Eq. (5) into a two-component topological BF field theory [88]:

$$S = i\int \frac{1}{2\pi}\mathscr{B}^T \wedge K\, d\mathscr{A} + i\int \frac{1}{2\pi}\mathbf{q}^T \mathscr{B} \wedge dA + \mathcal{S}_{ex}, \tag{31}$$

where we define the two-component vectors $\mathscr{B} = (\mathcal{B}, \mathcal{B}')^T$ and $\mathscr{A} = (\tilde{a}, \tilde{b})^T$, and use a differential form notation. Here, $\mathcal{B}$ and $\mathcal{B}'$ are two Kalb-Ramond 2-form gauge fields introduced as a result of the particle-vortex line duality transformation in (3+1)D [89]. Physically, they are related to the supercurrents of the condensates φ_1 and φ_2, respectively, via $J^{\varphi_1} = \frac{1}{2\pi} \star d\mathcal{B}$, $J^{\varphi_2} = \frac{1}{2\pi} \star d\mathcal{B}'$, where $\star$ is the usual Hodge-dual operation. Since the energy gap in the bulk of the topological BF field theory is effectively infinite, the term $\mathcal{S}_{ex}$ is added by hand in order to take into account the pointlike excitations labeled by $\mathbf{N}_m = (N_m^a, N_m^b)^T$, and the loop excitations labeled by the integer vector $\mathbf{L} = (\ell, \ell')^T$ (see Definition 1):

$$\mathcal{S}_{ex} = i\int \mathbf{N}_m^T \mathscr{A} \wedge \star j + i\int \mathbf{L}^T \mathscr{B} \wedge \star\Sigma, \tag{32}$$

where the vector j denotes the composite excitation current, and the tensor Σ denotes the loop excitation current. Integrating out the dynamical fields $\mathscr{A}$ and $\mathscr{B}$ yields an effective theory for j and Σ in the presence of the external EM field A_μ:

$$S_{\text{eff}} = i\mathbf{N}_m^T K^{-1}\mathbf{q}\int j \wedge \star A + i2\pi \mathbf{N}_m^T K^{-1}\mathbf{L}\int \Sigma \wedge d^{-1} j. \tag{33}$$

It is remarkable that the first term in the effective action (33) is nothing but the Debye screening charge cloud Q_{Debye} defined in Eq. (29). Thus, Q_{Debye} is a topological property of an excitation. The second term represents the long-range Aharonov-Bohm statistical interaction between fluxes and particles. The operator d^{-1} is a formal notation defined as the operator inverse of d, whose exact form can be understood in momentum space by Fourier transformation. The coefficient $\mathbf{N}_m^T K^{-1}\mathbf{L}$ gives rise to the charge-loop braiding statistics ϑ^{cl} between composite particles with quantum number $\mathbf{N}_m$ and loop excitations with electric fluxes $\Phi_e = 2\pi(K)^{-1}\mathbf{L}$ due to Eq. (22):

$$\vartheta^{cl} = 2\pi \mathbf{N}_m^T K^{-1}\mathbf{L} = \mathbf{N}_m^T \Phi_e. \tag{34}$$

Now that we have carefully developed a theory that describes topological phases in the presence of U(1) composite condensates, we will use the results to construct fractionalized 3D topological insulators with time-reversal symmetry.

III. FRACTIONAL TOPOLOGICAL INSULATORS

In this section, we will study 3D topological phases of matter with nonvanishing axion angle Θ. The presence of nontrivial values of Θ leads to several observable phenomena including a surface quantum Hall effect and the celebrated Witten effect: a magnetic monopole will bind a electric charge. For free-fermion time-reversal-invariant topological insulators, the angle is π mod 2π [59]. In fractionalized states where strong interactions and correlations are taken into account, in principle, the axion angle can be fractional (i.e., Θ/π is not integral) while time-reversal invariance is still maintained [35,68–71]. Such topological phases are called "fractional topological insulators" (FTI). In Ref. [68], FTIs were obtained via parton constructions where the partons themselves carry fractional EM electric charges, and the internal gauge fields are in the Coulomb phase where gauge fluctuations are weak and the photon(s) are gapless. In a different nonfractionalized state where $\mathrm{U}(1)\times\mathrm{U}(1)\rtimes Z_2$ symmetry is considered [90], the Θ term may signal a mutual Witten effect where a monopole of one U(1) gauge group induces an electric charge of another U(1) gauge group.

In the following, we will explore FTIs via the parton construction introduced in Sec. II. However, in Sec. III A, we shall first study charge lattices for which all partons occupy topological insulator bands and the internal gauge fields are in the Coulomb phase. The resulting state is a nonfractional topological insulator (i.e., $\Theta=\pi$) and there are two massless gauge bosons in the bulk. In order to obtain a gapped bulk and a fractional Θ, in Sec. III B we again assume that all partons occupy topological insulator bands and then we condense certain composites (see φ_1 and φ_2 of FTI in Table I). We focus on a concrete example and show that the resulting state is a FTI with time-reversal symmetry and $\Theta=\frac{\pi}{9}$ [cf. Eq. (57)]. As a side result, in Appendix C 1, we show that the *Ansätze* in which all partons are in a topologically trivial band structure always gives a topologically trivial state with $\Theta=0$ regardless of the condensate structure.

A. Topological insulators in the Coulomb phase

In the following, we consider partons occupying nontrivial 3D topological insulator bands (i.e., $\theta=\pi$). Previously, it was shown that partons with $\theta=\pi$ can potentially support a fractional Θ angle if the Coulomb phase is considered, and a special parton representation of an electron is used [68]. In the Coulomb phase, the dynamical gauge fields a_μ and b_μ are weakly fluctuating and noncompact; hence, the standard perturbative analysis is applicable. Integrating out the partons to quadratic order in the gauge fields [59], we obtain the following effective action S_{eff}:

$$\begin{aligned}S_{\text{eff}}=&\int d^4x\,\frac{\theta}{32\pi^2}\left(g_a f^a_{\mu\nu}+eG_{\mu\nu}\right)\left(g_a f^a_{\lambda\rho}+eG_{\lambda\rho}\right)\epsilon^{\mu\nu\lambda\rho}\\&+\int d^4x\,\frac{\theta}{32\pi^2}\left(-g_a f^a_{\mu\nu}-g_b f^b_{\mu\nu}+eG_{\mu\nu}\right)\\&\times\left(-g_a f^a_{\lambda\rho}-g_b f^b_{\lambda\rho}+eG_{\lambda\rho}\right)\epsilon^{\mu\nu\lambda\rho}\\&+\int d^4x\,\frac{\theta}{32\pi^2}\left(g_b f^b_{\mu\nu}-eG_{\mu\nu}\right)\\&\times\left(g_b f^b_{\lambda\rho}-eG_{\lambda\rho}\right)\epsilon^{\mu\nu\lambda\rho}+S_{\text{Maxwell}}\,,\end{aligned}\tag{35}$$

where $\theta=\pi$. The quantities $f^a_{\mu\nu}=\partial_\mu a_\nu-\partial_\nu a_\mu$ and $f^b_{\mu\nu}=\partial_\mu b_\nu-\partial_\nu b_\mu$ are field strength tensors of a_μ and b_μ, respectively. Both a_μ and b_μ are smooth variables and do not support monopole configurations. $G_{\mu\nu}$ is defined as $G_{\mu\nu}=F_{\mu\nu}-\frac{2\pi}{e}S_{\mu\nu}$, where $F_{\mu\nu}=\partial_\mu A_\nu-\partial_\nu A_\mu$, A_μ is smooth external EM field, and the tensor $S_{\mu\nu}$ forms the EM monopole current via $M_\mu=\frac{1}{2}\epsilon^{\mu\nu\lambda\rho}\partial_\nu S_{\lambda\rho}$. The constant e^2 denotes the fine-structure constant of the EM field A_μ. The coupling constants $g_{a,b}$ of the a_μ and b_μ gauge fields are written explicitly and $0<g_a,g_b\ll 1$ in the Coulomb phase. S_{Maxwell} includes all nontopological terms (Maxwell-type) of a_μ, b_μ, and A_μ. Since both a_μ and b_μ are smooth variables, all terms of the form $f^a\wedge f^a$, $f^a\wedge f^b$, and $f^b\wedge f^b$ are total-derivative terms that can be neglected in the bulk effective field theory. The term $-\frac{4\theta\, e\, g_b}{32\pi^2}f^b_{\mu\nu}G_{\lambda\rho}\epsilon^{\mu\nu\lambda\rho}=\frac{\theta g_b}{\pi}M_\mu b_\mu$ implies that M_μ carries integer gauge charge of the $\mathrm{U}(1)_b$ gauge group by noting that $\frac{\theta}{\pi}=1$. As such, after integrating a_μ,b_μ S_{eff} reduces to

$$S_{\text{eff}}=\frac{\Theta e^2}{32\pi^2}\int d^4x\,G_{\mu\nu}G_{\lambda\rho}\epsilon^{\mu\nu\lambda\rho}+\cdots\,,\tag{36}$$

where $\Theta=3\pi$. The terms represented by the ellipsis include the long-range Coulomb interactions between the monopole currents M_μ mediated by the b_μ photons, and other nontopological terms. Since the periodicity of Θ is still 2π in the absence of charge fractionalization, Θ reduces to π by a 2π periodic shift. In summary, the resulting state shows a Θ angle that is the same as a free-fermion topological insulator. The bulk admits two gapless, electrically neutral excitations, i.e., photons of the $\mathrm{U}(1)_a$ and $\mathrm{U}(1)_b$ gauge fields.

B. Fractional topological insulators in the composite condensation phase

The charge lattice in Sec. III A was obtained from the assumptions that (i) partons occupy $\theta=\pi$ topological insulator bands, and (ii) the internal gauge fields are in the Coulomb phase. However, the resulting phase supports a nonfractional $\Theta=\pi$ angle and the bulk spectrum is gapless. In the following, we consider composite condensation phases as discussed in Sec. II instead of the Coulomb phase. When the partons are in topological insulator bands, the resulting phase can support fractionalized Θ angles and a *fully* gapped bulk.

Let us start with the scenario that all partons occupy topological insulator bands (i.e., $\theta=\pi$) and then consider composite condensations. One can prove that parameters u,v,u',v',q,q' must be even,

$$u,v,u',v',q,q'\in\mathbb{Z}_{\text{even}}\,,\tag{37}$$

in order to satisfy the set of constraints given by Eqs. (8) and (12). We obtain the following relations via Eqs. (2)–(4) ($\theta=\pi$):

$$n^{f1}-n^{f2}=N_a-N^a_m-\tfrac{1}{2}N^b_m,\tag{38}$$

$$n^{f3}-n^{f2}=N_b-N^b_m-\tfrac{1}{2}N^a_m+M,\tag{39}$$

$$n^{f1}+n^{f2}-n^{f3}=N_A+N^b_m-\tfrac{3}{2}M.\tag{40}$$

In order to see whether or not there is charge fractionalization (Definition 2), we may check the value of Q defined in Eq. (28) when $M=0$. Then, Eq. (40) indicates that N_A is always

integer valued when $M=0$ by noting that n^{fi} and N_m^b are integer valued.

Thus, we should further check whether or not Q_{Debye} defined in Eq. (29) is fractional when $M=0$. In principle, one may deduce Θ as a function of the parameters (u,v,u',v',q,q',θ). However, such a generic discussion is technically intricate and not illuminating. Instead, we will proceed further with a concrete example as a proof of principle (see Table I): $u=2$, $v=2$, $u'=4$, $v'=10$, $q=2$, $q'=2$. In terms of the matrix notation defined in Eq. (14), we have

$$K=\begin{pmatrix}2 & 2\\ 4 & 10\end{pmatrix},\quad \mathbf{q}=\begin{pmatrix}2\\ 2\end{pmatrix}. \tag{41}$$

From Table I, we see that φ_1 is a bosonic bound state of two a_μ magnetic monopoles, two b_μ magnetic monopoles, one f^1 parton, four f^2 partons, and one f^3 parton. φ_2 is a bosonic bound state of four a_μ magnetic monopoles, ten b_μ magnetic monopoles, nine f^2 partons, and three holelike f^3 partons.

By using Eq. (24), it is straightforward to work out the relation between $N_{a,b}$ and M:

$$N_a=\tfrac{4}{3}M,\quad N_b=-\tfrac{1}{3}M, \tag{42}$$

which must be satisfied for all excitations. Plugging Eq. (42) into Eqs. (38) and (39), we end up with

$$n^{f1}-n^{f2}=\tfrac{4}{3}M-N_m^a-\tfrac{1}{2}N_m^b, \tag{43}$$

$$n^{f3}-n^{f2}=\tfrac{2}{3}M-N_m^b-\tfrac{1}{2}N_m^a. \tag{44}$$

It is obvious that the single parton f^i whose charges are shown in Table I is confined since Eqs. (43) and (44) are not satisfied simultaneously.

By noting that n^{fi},N_m^a,N_m^b,M are integer valued, Eqs. (43) and (44) require that

$$N_m^a,N_m^b\in\mathbb{Z}_{\text{even}};\quad M=0,\pm3,\pm6,\pm9,\ldots. \tag{45}$$

Therefore, the quantization of M is modified compared to the usual quantization $M=0,\pm1,\pm2,\ldots$ found in the vacuum and a nonfractionalized TI. A direct consequence is that an $M=1$ particle is not allowed to pass through the FTI, which is illustrated in Fig. 4.

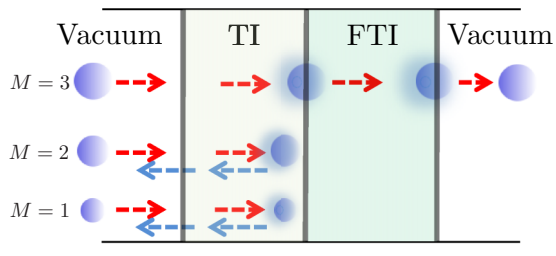

FIG. 4. Throwing three external EM magnetic monopoles (denoted by blue balls) in vacuum into topological materials TI and FTI. Only the EM magnetic monopole with $3k$, $k\in\mathbb{Z}$, magnetic charge shown in Eq. (45) can penetrate the FTI boundary in our example. An EM magnetic monopole with $M=1,2$ will be completely reflected on the FTI boundary, as shown by the leftward arrows. The shadow of each ball pictorially denotes the polarization charge cloud induced by the Witten effect.

We may use n^{f1}, n^{f2}, n^{f3}, and M to uniquely label all excitations. Solving Eqs. (43) and (44) gives rise to

$$N_m^a=\tfrac{4}{3}M-\tfrac{4}{3}n^{f1}+\tfrac{2}{3}n^{f2}+\tfrac{2}{3}n^{f3}, \tag{46}$$

$$N_m^b=\tfrac{2}{3}n^{f1}+\tfrac{2}{3}n^{f2}-\tfrac{4}{3}n^{f3}. \tag{47}$$

By using the above two equations, N_A in Eq. (40) and Q_{Debye} in Eq. (29) can be expressed as

$$N_A=\tfrac{1}{3}n^{f1}+\tfrac{1}{3}n^{f2}+\tfrac{1}{3}n^{f3}+\tfrac{3}{2}M, \tag{48}$$

$$Q_{\text{Debye}}=-2n^{f1}+\tfrac{2}{3}n^{f2}+\tfrac{4}{3}n^{f3}+\tfrac{16}{9}M. \tag{49}$$

The net EM electric charge Q is defined as N_A-Q_{Debye} and thus is given by

$$Q=\tfrac{7}{3}n^{f1}-\tfrac{1}{3}n^{f2}-n^{f3}-\tfrac{5}{18}M. \tag{50}$$

Thus, the quantization of Q is given by (see Appendix C 2)

$$Q=0,\pm\tfrac{1}{3},\pm\tfrac{2}{3},\pm1,\ldots\quad\text{when}\ \tfrac{M}{3}=0,\pm2,\ldots, \tag{51}$$

$$Q=0,\pm\tfrac{1}{6},\pm\tfrac{3}{6},\pm\tfrac{5}{6},\ldots\quad\text{when}\ \tfrac{M}{3}=\pm1,\pm3,\ldots. \tag{52}$$

Equation (51) indicates that the intrinsic excitations of the FTI (Definition 3) carry $\frac{1}{3}$ quantized EM electric charge. In other words, the FTI bulk supports charge fractionalization (Criterion 2). Due to the quantization of M in Eq. (45), Criterion 3 is automatically satisfied.

Equation (52) indicates that the 2D (M,Q) lattice is tilted by an angle $\frac{5}{18}M$. More precisely, an axion angle Θ can be defined as $\Theta=-\frac{5}{9}\pi$ by identifying $-\frac{5}{18}M=\frac{\Theta}{2\pi}M$. This M-dependent EM electric charge is a known consequence of the Witten effect [58,59,67].

The self-statistics of excitations (i.e., either fermionic or bosonic) can also be derived as a function of (n^{f1},n^{f2},n^{f3},M). For this purpose, let us start with Γ defined in Eq. (11) and take Eq. (45) into account. Therefore, the first two terms of Eq. (11) are even and can be removed, giving

$$\Gamma=(M+1)(n^{f1}+n^{f2}+n^{f3}), \tag{53}$$

where $-n^{f3}$ is also changed to n^{f3} leaving the even-odd property of Γ unaltered. In analogy to a TI, time-reversal symmetry should also be maintained. From the point of view of the charge lattice, time-reversal symmetry is a reflection symmetry $M\to-M$ that keeps the net EM electric charge and self-statistics invariant: $Q\to Q$, $\Gamma\to\Gamma+$ even integer. One possible definition of time-reversal symmetry that satisfies these properties is as follows:

$$\mathcal{T}n^{f1}\mathcal{T}^{-1}=n^{f1}-\tfrac{1}{3}M,\quad \mathcal{T}n^{f2}\mathcal{T}^{-1}=n^{f2}-\tfrac{2}{3}M, \tag{54}$$

$$\mathcal{T}n^{f3}\mathcal{T}^{-1}=n^{f3},\quad \mathcal{T}M\mathcal{T}^{-1}=-M, \tag{55}$$

where $\mathcal{T}$ denotes the time-reversal operator. It can be verified that Q is invariant and Γ is only changed by an even integer, thus leaving its even-odd property unaltered. Using the above transformations, we may also derive the transformations below:

$$\mathcal{T}N_m^a\mathcal{T}^{-1}=N_m^a-\tfrac{8}{3}M,\quad \mathcal{T}N_m^b\mathcal{T}^{-1}=N_m^b-\tfrac{2}{3}M. \tag{56}$$

The shifted amounts $-\frac{8}{3}M$ and $-\frac{2}{3}M$ are even integers, which guarantees the transformed $N_m^{a,b}$ are still even as required by Eq. (45). A time-reversed excitation is still an excitation, in

the sense that the transformed electric and magnetic charges also satisfy all equations that are satisfied by the excitation before time reversal. Geometrically, this means that after the above transformations, the new particle is still on the 4D charge lattice. Furthermore, Q and Γ are unchanged. From this geometric point of view, the time-reversal symmetry defined above effectively acts like a subgroup of the point group of the 4D charge lattice.

An important result is that the FTI with $\Theta = -\frac{5}{9}\pi$ is actually topologically equivalent to the FTI with $\Theta = \frac{1}{9}\pi$ by a periodic shift. The minimal choice of Θ for our FTI phase is given by

$$\Theta = \tfrac{1}{9}\pi \bmod \tfrac{2}{9}\pi. \tag{57}$$

To understand this result, let us revisit the self-statistics Γ in Eq. (53). In fact, Γ can be reformulated as a unique function of M and Q (see Appendix C 2 for details):

$$\Gamma = 3(M+1)\left(Q - \frac{\Theta}{2\pi}M\right), \tag{58}$$

where Θ is given by Eq. (57). We manifestly see that the even-odd property of Γ is unaltered by the *minimal* shift $\Theta \to \Theta + \frac{2}{9}\pi$. Γ is pictorially illustrated in Fig. 5(b) and we can see that geometrically, Θ describes how tilted the charge lattice is with respect to its initial orientation [Fig. 5(a)]. To illustrate, the red dashed line in Fig. 5(b) can be either more or less tilted with respect to the vertical axis via a shear deformation. The charge lattice [Fig. 5(b)] with a nonzero Θ can be obtained through such a shear deformation from the nontilted charge lattice [Fig. 5(a)]. Since $\Theta = \frac{1}{9}\pi$, the charge lattice shown in Fig. 5(b) is time-reversal invariant ($Q \to Q, M \to -M, \Gamma \to \Gamma +$ even integer), which can be viewed as a reflection symmetry about Q axis.

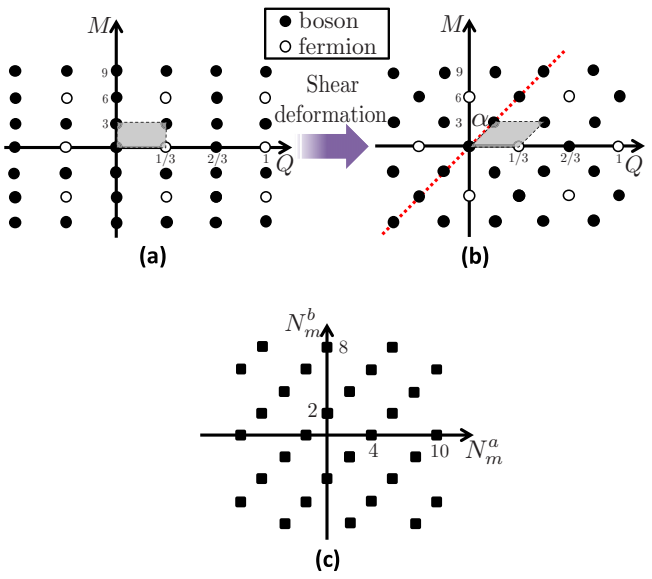

FIG. 5. Self-statistics distribution on the 4D charge lattice. (a) Self-statistics distribution as a function of M and Q by turning off Θ in Eq. (58). (b) Self-statistics distribution as a function of M and Q as shown in Eq. (58). The allowed values of M and Q are determined by Eqs. (51) and (52). Geometrically, $\Theta = 2\pi\tan\alpha$, where $\tan\alpha = \frac{1/6}{3} = \frac{1}{18}$. Thus, Θ angle can be viewed as a consequence of a shear deformation from (a) to (b). During the shear deformation, the area of "Dirac unit cell" (denoted by the shaded area) is invariant. Since the charge lattice is 4D (Definition 2), each site in (b) on the $(M-Q)$ parameter space corresponds to more than one excitation. An example is shown in (c), where N_m^a, N_m^b are used to label excitations that have the same Q and M: $Q = \frac{1}{6}$, $M = 3$.

It is obvious that the entire charge lattice [Fig. 5(b)] as well as the self-statistics distribution is unaltered if we further increase Θ by $\frac{2}{9}\pi$ (i.e., increase $\tan\alpha$ by $\frac{1}{9}$). For this reason, Θ is well defined only mod $\frac{2}{9}\pi$ as shown in Eq. (57). For example, the bosons on the site $(\frac{1}{6},3)$ are shifted to the bosons on the site $(\frac{1}{2},3)$; the fermions on the site $(0,6)$ are shifted to the fermions on the site $(\frac{2}{3},6)$. Furthermore, since the charge lattice is actually four dimensional (Definition 2), each lattice site of Fig. 5(b) actually corresponds to many excitations that are different from each other by N_m^a, N_m^b as shown in Fig. 5(c) where $Q = \frac{1}{6}, M = 3$ is illustrated. The lattice sites in Fig. 5(c) follow a simple relation: $(N_m^b - N_m^a - 1)/3 \in \mathbb{Z}$ where N_m^a, N_m^b are even (see Appendix C2 for details). More concrete examples of excitations including the original electrons are collected in Table II.

Experimentally, one may understand the physics of Θ via the surface quantum Hall effect on a surface with broken time-reversal symmetry. For example, by placing a ferromagnetic thin film on top of the surface of a FTI, we may observe a Hall effect with Hall conductance $\sigma_H = \frac{\Theta}{2\pi}\frac{e^2}{h}$ [59]:

$$\sigma_H = \left(\frac{1}{18} + \frac{n}{9}\right)\frac{e^2}{h}, \quad n \in \mathbb{Z} \tag{59}$$

where h is the usual Planck constant. It should be kept in mind that, although the minimal nonzero σ_H is $\frac{1}{18}$, the

TABLE II. Examples of excitations in our FTI. The electric and magnetic charges are explicitly shown. "F" is short for "fermionic" where Γ is odd. "B" is short for "bosonic" where Γ is even. We call an elementary charge an intrinsic excitation (Definition 3) that carries $Q = \frac{1}{3}$ or $Q = \frac{2}{3}$ EM electric charge, in analogy to the fractionalized charge excitations in the $\nu = \frac{1}{3}$ FQH state. The two elementary charges in the table are just two concrete examples, and there are many other excitations that carry $Q = \frac{1}{2}, \frac{2}{3}$ and $M = 0$. The elementary EM monopole is an excitation that carries the minimal nonzero EM magnetic charge $M = 3$ and does not contain any partons (i.e., $n^{fi} = 0, \forall\, i = 1,2,3$). A nonzero M can be externally added into the bulk in order to probe the EM response (see Definition 3). The minimal quantum of charge fractionalization is $\frac{1}{3}$ determined by the intrinsic excitations, i.e., Eq. (51) rather than Eq. (52).

	n^{f1}	n^{f2}	n^{f3}	M	N_A	Q_{Debye}	Q	N_m^a	N_m^b	Γ
Elementary charge	1	0	2	0	1	$\frac{2}{3}$	$\frac{1}{3}$	0	-2	F
Elementary charge	2	9	1	0	4	$\frac{10}{3}$	$\frac{2}{3}$	4	6	B
Electron	1	1	1	0	1	0	1	0	0	F
Elementary EM monopole	0	0	0	3	$\frac{9}{2}$	$\frac{16}{3}$	$-\frac{5}{6}$	4	0	B
An example with $M = 3$	1	1	1	3	$\frac{11}{2}$	$\frac{16}{3}$	$\frac{1}{6}$	4	0	B
An example with $M = 3$	2	1	0	3	$\frac{11}{2}$	2	$\frac{7}{2}$	2	2	B
An example with $M = 6$	1	1	1	6	10	$\frac{32}{3}$	$-\frac{2}{3}$	8	0	F
An example with $M = 6$	2	1	0	6	10	$\frac{22}{3}$	$\frac{8}{3}$	6	2	F

corresponding charge induced by the Hall response is not $\frac{1}{18}$ since the quantization of M in Eq. (45) is modified from its nonfractionalized value. More precisely, an external EM monopole with M magnetic charge can be viewed as $2\pi M$ EM magnetic fluxes threading the surface [91]. By using the Laughlin argument, the surface will generate $\frac{1}{18}M$ response charge once the EM monopole penetrates the surface. Since the minimal nonzero M is 3 due to Eq. (45), the minimal surface response charge is $\frac{1}{18}\times 3=\frac{1}{6}$ rather than $\frac{1}{18}$. Further, the $\frac{1}{6}$ charge will be attached onto the EM magnetic monopole that moves into the FTI bulk, which renders the Witten effect [58,59,67]. This phenomenon is nontrivial in a sense that the $\frac{1}{6}$ charge cannot be formed by the bulk intrinsic excitations (Definition 3) whose Q is quantized at $\frac{1}{3}$ due to Eq. (51).

An FTI can be viewed as a symmetry-enriched topological phase (SET) which is characterized by both bulk topological order (TO) data and a symmetry action. In our case, the latter is encoded by the structure of the charge lattice in Fig. 5. The former is given by the set of all intrinsic excitations (Definition 3, i.e., all sites along the Q axis in Fig. 5) and also loop excitations (Definition 1). With these preliminaries, we may discuss the consequence of stacking operations in the context of topological order [92,93]. Stacking operations, denoted as $\boxtimes$, form a monoid that does not contain inverse elements. It is known that stacking two TIs leads to the topologically trivial vacuum state: TI $\boxtimes$ TI = Vacuum. Let us stack a 3D TI and a 3D FTI together. The resulting phase is a TO: FTI $\boxtimes$ TI = TO. In other words, the stacking operation removes the nontrivial Witten effect of the FTI, rendering a state with pure topological order. This can be understood in two steps. First, since the bulk intrinsic excitations of a TI only contain electron excitations, the above stacking operation indeed does not change the TO of the FTI. Second, in the stacked phase, the net EM electric charge Q is given by $Q=(\frac{\pi}{18}M+\frac{n}{3})+(\frac{\pi}{2}M+n')$ with $n,n'\in\mathbb{Z}$, where the first term is given by the Witten effect of the FTI while the second term is given by the Witten effect of the TI. Since the stacked phase is formed by putting the FTI and TI in the same spatial 3D region, the quantization of M in Eq. (45) still holds in the stacked phase. As a result, the electric charge Q in the stacked phase is given by $Q=\frac{5}{9}M+\frac{n}{3}+n'$, where the M-induced charge $\frac{5}{9}M$ is quantized to $\frac{5}{3}$. This charge can be completely screened by $\frac{n}{3}+n'$, e.g., $n=-2$, $n'=-1$. Thus, the charge lattice of the stacked phase is not tilted, meaning that $\Theta=0$.

In summary, the stacking of a FTI and a TI leads to a phase with pure topological order where the Witten effect is absent. We may also consider stacking two FTIs: FTI $\boxtimes$ FTI = TO $\boxtimes$ TO, which means that the stacked phase is a purely topologically ordered phase where the charge lattice is not tilted and the topological order is given by TO $\boxtimes$ TO. Surely, this is just an example while it is possible that other examples of FTI may produce different phases when stacked together with TI or with themselves. Stacking operations in SET phases generally change TO to a new topological order denoted as "$\widetilde{\text{TO}}$." For example, stacking two FTIs here gives rise to $\widetilde{\text{TO}}=\text{TO}\boxtimes\text{TO}$. In order to see if the resulting phase is a new SET or not, one should further consider symmetry-respecting condensations that change $\widetilde{\text{TO}}$ back to TO. In this way, we may make progress toward the classification of SETs. As it is beyond the scope of this work, we will leave this issue to further studies.

The above calculation is based on concrete numerical inputs (41). As mentioned previously, one may in principle generically deduce Θ as a function of the parameters (u,v,u',v',q,q',θ) that fully determine the two permissible composite condensations and the entire bulk spectrum. In 2D, we know that some FQH states can be unified into Jain's sequence [60,61] such that they can be understood in the composite-fermion theory with different microscopic designs of the composite particles. Our 3D composite particle theory is similar to this 2D scenario: the Θ angle, and other properties of composite condensation phases, are also determined by the different designs of composite condensations. Therefore, all phases constructed from composite condensations can be thought to form a sequence. We expect more studies in the future along this line of thinking will be helpful in uncovering the physics of 3D Abelian topological phases of strongly interacting fermion systems.

C. Deconfined discrete gauge subgroup $\mathbb{Z}_2\times\mathbb{Z}_6$: Abelian topological order in the bulk

The FTI state obtained in Sec. III B supports fractionalized intrinsic excitations as indicated by Eq. (51) and the texts around it. Reference [71] has pointed out that FTIs necessarily have a fractionalized bulk. Therefore, our construction is consistent to the claim. Usually, a fractionalized gapped bulk can be understood as the presence of a topological order of some form. To see more clearly the exact form of the topological order of our FTI, let us start with the K matrix in Eq. (41). By using two independent unimodular matrices (i.e., Ω and W that will be discussed in details in Sec. IV), we may diagonalize K:

$$\Omega K W^T=\begin{pmatrix}2&0\\0&6\end{pmatrix}, \tag{60}$$

where

$$\Omega=\begin{pmatrix}1&0\\-2&1\end{pmatrix},\quad W=\begin{pmatrix}1&0\\-1&1\end{pmatrix}. \tag{61}$$

In the new basis, it is clear that the bosonic sectors of the ground state are described by deconfined $\mathbb{Z}_2\times\mathbb{Z}_6$ gauge group. In other words, the maximal torus U(1) × U(1) of the SU(3) gauge group of the parton construction is confined *except* the $\mathbb{Z}_2\times\mathbb{Z}_6$ gauge subgroup. In Ref. [71], the discrete gauge group $\mathbb{Z}_2$ arises since the choice of parton mean-field Hamiltonian explicitly breaks the original pseudospin SU(2) gauge group down to $\mathbb{Z}_2$ subgroup. However, in our FTI state, the discrete gauge subgroup arises from the the deconfined subgroup of a confined non-Abelian gauge group, physically due to the condensation of composites that contain magnetic monopoles.

IV. CHARGE-LOOP EXCITATION SYMMETRY AND ITS RELATION TO EXTRINSIC TWIST DEFECTS

In Sec. III, we have explored the axion angle of the charge lattice with composite condensation. In this section, we will explore the charge-loop excitation symmetry based on the composite particle theory introduced in Sec. II.

The topological BF field theory (31), which is derived from the two permissible composite condensates, only captures the statistical interaction between particles that carry N_m^a, N_m^b magnetic charges and loops that carry Φ_e^a, Φ_e^b electric fluxes. Specifically, several important properties of composites, such as the self-statistics Γ in Eq. (10), and the net EM electric charge Q in Eq. (28), are not encoded in Eq. (31). However, the topological BF field theory reproduces Q_{Debye}, an important part of Q. In this section, we further study the topological BF field theory and show that it serves as a useful platform to study "*char*ge-*l*oop *e*xcitation *s*ymmetry" (abbreviated as "Charles," see Definition 5) that can be viewed as a 3D generalization of "anyonic symmetry" [73] (or "topological symmetry" in Ref. [78] and references therein) in 2D Abelian topological phases. We expect that 3D Abelian topological phases where loop excitations are allowed may host even more exotic physics if extrinsic twist defects are imposed, and anticipate that 3D charge-loop excitation symmetry will be a useful tool in future studies of such extrinsic defects.

A. Definition of Charles

In 2D topological phases, each pointlike extrinsic twist defect is associated with an element of an anyonic symmetry group G. The anyonic symmetry group is a finite group that acts to permute a subset of anyons in the parent TO phase while preserving all of the topological properties (topological spin, statistics) of the anyons (and sometimes their symmetry properties as well, e.g., their EM charge). For example, the permutation of e and m particles in the 2D Wen-plaquette model (with $\mathbb{Z}_2$ TO) [94] is a typical anyonic symmetry transformation. For this particular model, this transformation can be realized by extrinsically imposing a lattice dislocation which enacts the permutation of e and m when an anyon passes through a 1D branch cut that terminates at the extrinsic point defect [73,79,84,95]. Interestingly, this quasiparticle permutation mechanism endows the dislocation with an attached non-Abelian object at the defect core, which opens up a possible new platform for topological quantum computation. Mathematically speaking, the incorporation of extrinsic defects into 2D Abelian topological phases described by a category theory $\mathcal{C}$ promotes $\mathcal{C}$ to a G-crossed tensor category theory $\mathcal{C}_G^\times$ [73,78].

Let us briefly recall some properties of anyonic symmetry in 2D Abelian topological phases. As mentioned, these phases are described using Abelian Chern-Simons theory using the data in a symmetric, integer K matrix. There are an important class of unimodular, integer transformations W satisfying $WKW^T = K$ that act as the automorphisms of K (or the automorphisms of the integer lattice, and dual/quasiparticle lattice, determined by K). These transformations relabel the different anyonic excitations, but most of them preserve the anyon type, and just attach local quasiparticles (e.g., attaching extra electrons). These trivial transformations are called the inner automorphisms Inner(K) and they form a normal subgroup of the full set of automorphisms Auto(K). The nontrivial anyonic relabeling symmetries are hence given by the group $G \equiv \text{Outer}(K) = \frac{\text{Auto}(K)}{\text{Inner}(K)}$. This captures the conventional anyonic symmetries that act as point-group operations on the quasiparticle lattice, although it leaves out possible nonsymmorphic lattice operations or symmetries of stably equivalent K matrices [73,74,96]. We will not consider these more complicated possibilities for anyonic symmetries any further and leave their 3D generalization to future work.

In order to generalize this discussion of anyonic symmetry and extrinsic defects to 3D, let us revisit some basic facts of excitations in our 3D fermionic gapped phase formed by two permissible composite condensates. The 2D vectors $\mathbf{L}$ form a 2D loop lattice in Definition 1. The 2D vectors $\mathbf{N}_m$ form a 2D lattice which is a sublattice of the 4D charge lattice in Definition 2. As a whole, we may define a 6D *charge-loop lattice*. (N.B., this is not the same 6D lattice mentioned earlier.)

Definition 4 (Charge-loop lattice). The charge-loop lattice is a 6D lattice whose sites are given by the 6D lattice vector $\vec{V} = (N_A, \mathbf{N}_m^T, M, \mathbf{L}^T) = (N_A, N_m^a, N_m^b, M, \ell, \ell')$. Each site corresponds to a *charge-loop composite*.

In order to avoid confusions in terminology, the word "composite," if used by itself, always denotes a pointlike particle, unless otherwise specified. The symmetry group Charles is then defined as below:

*Definition 5 (Charge-loop excitation symmetry (*Charles*)).* The charge-loop excitation symmetry group is a subset of the point group of the 6D charge-loop lattice and corresponds to the following quotient group:

$$\text{Charles} = \frac{\text{Auto}(K)}{\text{Inner}(K)}, \tag{62}$$

where Auto(K) is the group of generalized automorphisms of K. Inner(K) is the group of generalized inner automorphisms of K, which is a subgroup of Auto(K). Group elements of Auto(K) have the matrix representation $\mathscr{G} = W \oplus \Omega$, where the two independent rank-two unimodular matrices W and Ω satisfy the following two conditions:

$$\text{(i)} \quad \Omega K W^T = K, \tag{63}$$

$$\text{(ii)} \quad \Gamma(\ldots, \mathbf{N}_m, \ldots) = \Gamma(\ldots, W^{-1}\mathbf{N}_m, \ldots). \tag{64}$$

Here, Γ is the self-statistics of composites, which is a function of lattice sites labeled by the 4D coordinates $(N_A, \mathbf{N}_m^T, M)$. In addition to conditions (i) and (ii), the group elements in Inner(K) have the property that $W^{-1}\mathbf{N}_m - \mathbf{N}_m = K^T (n_1, n_2)^T$ and $\Omega^{-1}\mathbf{L} - \mathbf{L} = K(n_3, n_4)^T$, where $n_1, \ldots, n_4$ are integers. n_1 and n_2 are functions of $\mathbf{N}_m, W$; n_3 and n_4 are functions of $\mathbf{L}, \Omega$.

Just like the 2D anyonic symmetry group, the definition of Charles also involves the definitions of Auto(K) and Inner(K). One can prove that Auto(K) satisfies the usual group axioms (identity element, inverse element, closure, associativity) and that Inner(K) is a normal subgroup of Auto(K), such that Charles forms a group. Details of this proof can be found in Appendix D.

Physically, group elements $\mathscr{G} = W \oplus \Omega$ in Charles correspond to point-group transformations: $(\mathbf{N}_m)_{\text{new}} = W^{-1}\mathbf{N}_m$, $(\mathbf{L})_{\text{new}} = \Omega^{-1}\mathbf{L}$. Conditions (i) and (ii) guarantee that the transformed charge-loop lattice is identical to the original one, which means that Charles keeps not only the lattice geometry invariant, but also leaves all topological properties of particle excitations and loop excitations (denoted by lattice sites) unaffected. Those topological properties include the self-statistics of particle excitations Γ, the charge-loop braiding statistics ϑ^{cl}, and the Debye screening Q_{Debye}. However, there

is a redundancy corresponding to Inner(K) that should be removed. Inner(K) includes all trivial transformations whose point-group effects are equivalent to effectively shifting both $\mathbf{N}_m$ and $\mathbf{L}$ by undetectable amounts [i.e., $\vartheta^{cl} = 0 \bmod 2\pi$ in Eq. (34); see also Sec. II C], and thereby must be modded out from Auto(K) if we only want to keep nontrivial transformations. Again, the transformations in Inner(K) can be interpreted as changing the excitations by a trivial, topologically undetectable charge or flux.

In contrast to the 2D definition of "anyonic symmetry" where condition (i) (where the simpler structure only allows for $W = \Omega$) is enough to guarantee the invariance of the self-statistics of anyons, one now needs condition (ii) in order to guarantee that the self-statistics of excitations on the 4D charge lattice remains invariant under Charles transformations. The main reason for this is that the self-statistics of an excitation (Definition 2) cannot be captured by the topological BF field theory. *Whether or not W satisfies condition (ii) relies on the specifics of the parton decomposition, and in the following subsections, we will assume condition (ii) is satisfied.*

B. General theory of Charles and its tensor-network-type representation

It should be noted that W, Ω, and K in Definition 5 can be naturally generalized to arbitrary rank if a physical realization using a scenario having any number of permissible composite condensates in Sec. II A can be achieved. For example, one can consider a single composite condensate or three linearly independent condensates with entirely different parton constructions, which leads to a number $K \in \mathbb{Z}$ or a rank-three K matrix, respectively.

Before proceeding further, we introduce a simplified notation that will be useful for subsequent discussions. The notation in the two-component BF action (31), such as $\tilde{a}$ and $\tilde{b}$, comes from the specific physical realization described in Sec. II A. It is, however, inconvenient for the purpose of generalizing Charles. Thus, in the current section (Sec. IV B), we temporarily use a new notation for the gauge fields $b = (b^1, b^2, \dots)$ and $a = (a^1, a^2, \dots)$ where b is a set of 2-form Kalb-Ramond U(1) gauge fields while a is a set of 1-form U(1) gauge fields. As a result, the topological BF term is expressed as

$$\frac{iK^{IJ}}{2\pi}\int b^I \wedge da^J = \frac{i}{2\pi}\int b^T \wedge K da \qquad (65)$$

with a square matrix K of rank N. The excitation terms in Eq. (32) are rewritten as

$$\mathcal{S}_{ex} = i\int \mathbf{t}^T a \wedge \star j + i\int \mathbf{L}^T b \wedge \star\Sigma\,, \qquad (66)$$

where $\mathbf{t} = (t_1, t_2, \dots)$ is an integer vector replacing the notation $\mathbf{N}_m$. Then, the charge-loop lattice is formed by an N-dimensional charge lattice labeled by vectors $\mathbf{t}$ and an N-dimensional loop lattice labeled by vectors $\mathbf{L}$. Group elements of Charles are still denoted as "$\mathcal{G} = W \oplus \Omega$" with the transformations $(\mathbf{t})_{\text{new}} = W^{-1}\mathbf{t}$ and $(\mathbf{L})_{\text{new}} = \Omega^{-1}\mathbf{L}$.

Let us consider some examples. In Table III, all possible Charles groups are listed for a 1×1 matrix $K \in \mathbb{Z}$. From the table, we see that $\mathbb{Z}_2$ gauge theory in (3+1)D ($K = 2$) only has trivial Charles, which is surprisingly different from a deconfined $\mathbb{Z}_2$ gauge theory in (2+1)D (e.g., as appears in the Wen-plaquette model), where the $e \leftrightarrow m$ exchange process is an anyonic symmetry transformation. Nontrivial Charles arises for $\mathbb{Z}_K$ gauge theory in (3+1)D *only* when $|K| \geqslant 3$. For example, for $\mathbb{Z}_3$ gauge theory, the nontrivial element of Charles is $-\mathbb{I} \oplus -\mathbb{I}$ which means that $W = \Omega = -\mathbb{I}$ (here $\mathbb{I}$ reduces to the natural number "1"). Under the transformation of this group element, there is an exchange symmetry between a particle with one unit of gauge charge and a particle with two units of gauge charge since the latter is trivially equivalent to a particle with gauge charge -1. There is also an exchange symmetry between a loop with magnetic flux $2\pi/3$ and a loop with magnetic flux $4\pi/3$ ($= -\frac{2\pi}{3} + 2\pi$). These two exchange processes must occur *simultaneously*.

TABLE III. Examples of Charles (Sec. IV B) when the matrix K reduces to an integer. A generic group element is denoted by $\mathcal{G} = W \oplus \Omega$. $\mathcal{G}_{\mathbb{I}}$ denotes the identity element: $\mathcal{G}_{\mathbb{I}} = \mathbb{I} \oplus \mathbb{I}$.

K	Charles
$K = \pm 1$	$\{\mathcal{G}_{\mathbb{I}}\}$
$K = \pm 2$	$\{\mathcal{G}_{\mathbb{I}}\}$
$\lvert K\rvert \geqslant 3$	$\{\mathcal{G}_{\mathbb{I}}, -\mathbb{I} \oplus -\mathbb{I}\}$

A simple example of a rank-2 K matrix is $K = 2\sigma_x$. If we do not worry about Charles for a moment, a diagonalization can be achieved by using $W = \sigma_x, \Omega = \mathbb{I}_{2\times 2}$. In the new basis, we end up with two copies of the level-2 topological BF field theory, thereby obtaining a $\mathbb{Z}_2 \times \mathbb{Z}_2$ discrete gauge theory (i.e., $\mathbb{Z}_2 \times \mathbb{Z}_2$ topological order). Due to Definition 5, such a basis change is clearly not a group element of Charles, but it reveals that the gauge structure is $\mathbb{Z}_2 \times \mathbb{Z}_2$ rather than $\mathbb{Z}_4$. It is important to distinguish these possibilities since those two gauge structures produce the same ground state degeneracy (GSD) on a 3-torus [88,97–99]. For this example, a typical group element of Charles is $\mathcal{G} = \sigma_x \oplus \sigma_x$, which satisfies condition (i) in Eq. (63). Physically, Ω exchanges a particle labeled by $\mathbf{t} = (0,1)^T$ and a particle labeled by $\mathbf{t} = (1,0)^T$. At the same time, Ω exchanges a loop labeled by $\mathbf{L} = (0,1)^T$ and a loop labeled by $\mathbf{L} = (1,0)^T$.

For convenience, condition (i) in Eq. (63) can be visually represented by a tensor-network-type graph as shown in Fig. 8(a) of Appendix D. It indicates that K is a fixed-point tensor (here, a matrix) that is invariant under Charles renormalization-group-like transformations. The bond dimension is given by the rank of K. This graphical representation allows us to straightforwardly generalize the notion of Charles to more general Abelian topological quantum field theories (TQFTs) in (3+1)D that include more exotic topological terms. For instance, let us consider a TQFT with the action

$$S = \frac{i}{2\pi}\int b^T \wedge K da + i\int \Lambda^{IJK} a^I \wedge a^J \wedge da^K\,, \qquad (67)$$

where Λ^{IJK} is a real tensor with three legs as shown in Fig. 8(b) of Appendix D. By itself, and at a classical level, the second term in this action corresponds to a topological invariant for the mutual linkage of three electromagnetic flux loops [100]. At a quantum level, the action S was also proposed as a

continuum field theory description of Dijkgraaf-Witten lattice gauge theory [101,102]. It can also be derived by gauging the global onsite symmetry group $G = \mathbb{Z}_{N_1} \times \mathbb{Z}_{N_2} \times \cdots$ of the TQFT action of a 3D SPT phase with $N_1 \times N_2 \times \cdots = |\det K|$, where the quantization of Λ^{IJK} is determined by the number of topologically distinct ways to impose G in SPT phases [103]. The relation to three-loop statistics [104–106] is being investigated [103,104,107]. It is believed that the coefficient Λ^{IJK} encodes the information of three-loop statistics that classifies topologically distinct twisted discrete Abelian gauge field theories in (3+1)D. In analogy to the topological BF field theory, the tensor Λ^{IJK} must also be transformed accordingly under the charge-loop-lattice point-group transformations. In order to keep the important three-loop statistics data [104] invariant, the generalized Charles should incorporate the following condition:

$$\sum_{I'J'K'} W^{I'I} W^{J'J} W^{K'K} \Lambda^{I'J'K'} = \Lambda^{IJK} \tag{68}$$

in addition to those conditions in Definition 5. Likewise, we can also use a tensor-network-type graph [Fig. 8(b) of Appendix D] to graphically represent Eq. (68), where the bond dimension is no less than two.

Finally, we can also consider a TQFT with the action

$$S = \frac{i}{2\pi} \int b^T \wedge K\, da + i \int \Xi^{IJKL} a^I \wedge a^J \wedge a^K \wedge a^L, \tag{69}$$

where the coefficient Ξ^{IJKL} is a tensor with four legs. Likewise, the quantized values of Ξ encode the information of the four-loop braiding process [105] and can provide topological invariants for classifying twisted discrete gauge field theories in (3+1)D. In order to keep Ξ invariant under point-group transformations of the charge-loop lattice, the following relation should be obeyed:

$$\sum_{I'J'K'L'} W^{I'I} W^{J'J} W^{K'K} W^{L'L} \Xi^{I'J'K'L'} = \Xi^{IJKL}. \tag{70}$$

A tensor-network-type representation is shown in Fig. 8(c) of Appendix D, where the bond dimension is no less than four.

We may also consider the scenario that Charles transformations can be performed *locally* so that Charles becomes dynamically *gauged*. In this case, the extrinsic twist defects become well defined, deconfined excitations of a new topological phase. The resulting phases have been thoroughly studied in 2D and are non-Abelian topological phases called twist liquids [73–84]. As a result, W and Ω become space-time dependent. The difference between the next-nearest lattice sites is compensated by locally twisting matter fields. The tensor-network graph representations of the various symmetry transformations in Fig. 8 of Appendix D are suggestive that such a tensor-network analysis may be a useful tool for future studies of 3D twist liquids.

C. Theory of Charles defects: Twist defect species and fusion

In the following, we study extrinsic twist defects associated with Charles group elements in analogy to extrinsic twist defects in 2D Abelian topological phases with anyonic symmetry [73,74,77–81,84]. More specifically, we explore two issues: (i) the universal labeling of a defect in 3D, and (ii) the fusion properties of defect-charge-loop composites. Recently, remarkable progress in the study of various aspects of string/loop excitations in (3+1)D topological phases of matter, such as their description using lattice models and field theories, their associated ground-state degeneracy (GSD), and their braiding and fusion properties has been made [75,92,104,108–117]. As will be seen below, the consideration of extrinsic defects within the framework of charge-loop excitation symmetry introduces a new aspect to the physics of loop excitations in (3+1)D topological phases.

We begin by reviewing the physics of twist defects and defect-anyon composites in 2D Abelian topological phases. From a topological point of view, externally imposed defects in such phases are a set of special, potentially non-Abelian objects. For Abelian groups, each group element of the anyonic symmetry group G corresponds to a bare defect and there are $\mathrm{ord}(G)$ distinct bare defects, where $\mathrm{ord}(G)$ is the order of G. Generically, the defects are labeled by the conjugacy classes of G, but since we only deal with Abelian groups here we will not often make this distinction. By a "bare" defect, we really mean that the defect is externally imposed alone in the bulk. In general, defects can be bound to anyons of the parent Abelian topological phase, thereby forming a *defect-anyon composite* which is, by definition, not bare. When given a group element of G, the total number of topologically distinct defects (also known as defect species) includes bare ones and composite ones, and is not always the same as the number of topologically distinct anyons. In other words, two defect-anyon composites might be topologically equivalent to each other if there do not exist gauge-invariant Wilson measurements that can distinguish them. Indeed, there is a consistency equation for determining the equivalence classes of defect types [73,74]

$$\mathcal{D}^0_{\mathscr{G}} \times qp = \mathcal{D}^0_{\mathscr{G}} \times [qp + (\mathbb{I} - \mathscr{G}) qp_1], \tag{71}$$

which is diagrammatically shown in Fig. 7(a). Here, qp denotes a quasiparticle (i.e., an anyon) that is provided by the parent 2D Abelian topological phase. $\mathcal{D}^0_{\mathscr{G}}$ denotes a bare defect labeled by a group element $\mathscr{G}$ of the anyonic symmetry group G. The particle qp_1 is any anyon provided by the parent 2D Abelian topological phase. The composite object $\mathcal{D}^0_{\mathscr{G}} \times qp$ denotes the fusion between $\mathcal{D}^0_{\mathscr{G}}$ and qp that forms a defect-anyon composite. Specifically, Eq. (71) determines when this defect-anyon composite is topologically identical to a defect-anyon composite that is formed by the fusion between the same bare defect and a different anyon given by $qp + (\mathbb{I} - \mathscr{G}) qp_1$. The symbol "+" should be regarded as the addition of quasiparticle vectors in the K-matrix Chern-Simons theory. The physical reason of this equivalence is really due to the nontrivial internal structure of a defect-anyon composite. More specifically, the anyon qp that is trapped at the defect can emit anyon qp_1 which moves around the defect once. As a result, anyon qp_1 is changed to anyon $\mathscr{G} qp_1$ that is finally absorbed by the defect. Such a process occurs inside the defect-anyon composite and cannot change the defect species [74]. Therefore, the process provides an equivalence between two defect-anyon composites.

A typical example in (2+1)D is $K = 2\sigma_x$ Chern-Simons theory that describes $\mathbb{Z}_2$ topological order. Its anyonic

symmetry group is given by $\{\mathbb{I},\sigma_x\}$. The nontrivial group element σ_x interchanges the anyon e, labeled by the quasiparticle vector $(1 \bmod 2, 0 \bmod 2)^T$, and the anyon m, labeled by the quasiparticle vector $(0 \bmod 2, 1 \bmod 2)^T$. A defect labeled by this group element can in principle be realized by externally imposing a dislocation in the Wen-plaquette model as mentioned previously. For convenience, the identity quasiparticle (vacuum) vac is labeled by $(0 \bmod 2, 0 \bmod 2)^T$, and the fermion quasiparticle ψ is labeled by $(1 \bmod 2, 1 \bmod 2)^T$. Thus, the only non-trivial, bare defect is given by $\mathcal{D}^0_{\sigma_x}$. Next, we need to deduce equivalence classes of defect-anyon composites. Taking into account Eq. (71) and $\mathbb{I} - \sigma_x = \left(\begin{smallmatrix} 1 & -1 \\ -1 & 1 \end{smallmatrix}\right)$, we have

$$\mathcal{D}^0_{\sigma_x} \times qp = \mathcal{D}^0_{\sigma_x} \times (qp + \epsilon), \quad \forall\, qp \in \{\text{vac}, e, m, \epsilon\}.$$

Here, the symbol "+" denotes the usual addition of quasiparticle vectors of qp and ϵ. Therefore, there are two equivalence classes: $\mathcal{D}^0_{\sigma_x} \times e = \mathcal{D}^0_{\sigma_x} \times m$ and $\mathcal{D}^0_{\sigma_x} \times \psi = \mathcal{D}^0_{\sigma_x}$. In other words, there are two topologically distinct defects: one is bare, given by a bare defect $\mathcal{D}^0_{\sigma_x}$; the other one is a defect-anyon composite, denoted by $\mathcal{D}^1_{\sigma_x} = \mathcal{D}^0_{\sigma_x} \times e$. The fusion rules of these two defects are given by

$$\mathcal{D}^0_{\sigma_x} \times \mathcal{D}^0_{\sigma_x} = \mathcal{D}^1_{\sigma_x} \times \mathcal{D}^1_{\sigma_x} = \text{vac} + \psi, \quad \mathcal{D}^0_{\sigma_x} \times \mathcal{D}^1_{\sigma_x} = e + m,$$

where "+" here denotes the collection of different fusion channels into quasiparticles of simple type.

Now that we have reviewed the lower-dimensional case, let us move on to 3D. Simply from a dimensionality point of view, there are two types of extrinsic defects in 3D: line defects and point defects. The latter also appear in 2D and serve as end points on which 1D branch cuts [i.e., the dashed line in Fig. 6(b)] terminate. The former are really looplike. In Fig. 6(a), the line defect is drawn as a finite line that ends at the top and bottom boundaries where a periodic boundary condition is implicitly imposed. A 2D branch "brane" [i.e., the shaded plane in Fig. 6(a)] is attached to each line defect.

From Fig. 6, we see that line defects can perform generic Charles operations where both point particles and loops are transformed. In contrast, point defects can only perform Charles operations on loops, meaning that $\mathcal{G} = W \oplus \Omega = \mathbb{I} \oplus \Omega$ for point defects. However, due to Eq. (63), the only candidate for Ω is $\mathbb{I}$. This means that point defects can only behave like the identity element $\mathcal{G}_{\mathbb{I}} = \mathbb{I} \oplus \mathbb{I}$ of Charles. Therefore, in 3D, we only consider line defects since point defects *cannot* perform nontrivial Charles operations.

In a manner similar to 2D, a *defect-charge-loop composite* is allowed, where the term "defect" corresponds to a line defect, "charge" corresponds to a pointlike excitation, and "loop" corresponds to a loop excitation. Since loops are always transformed to loops by Ω, and particles are always transformed to particles by W, we may study defect-charge composites and defect-loop composites separately. In order to determine defect species for a given Charles group element $\mathcal{G}$, we need to study the equivalence classes of the above two kinds of defect composites. For defect-charge composites, the following equation determines the equivalence classes:

$$\mathcal{D}^0_{\mathcal{G}} \times qp = \mathcal{D}^0_{\mathcal{G}} \times [qp + (\mathbb{I} - W)qp_1], \tag{72}$$

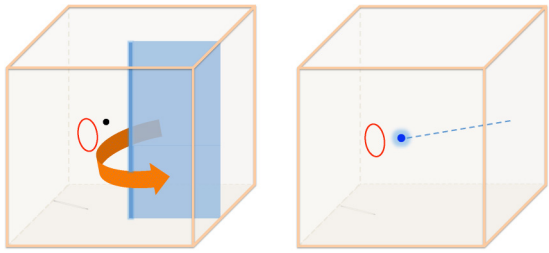

FIG. 6. Extrinsic twist defects in 3D. (a) Line defect; (b) point defect. The two cubic boxes denote the 3D bulk of an underlying quantum many-body system. The shaded plane in (a) denotes a 2D branch cut/plane ending at the line defect, while the dashed line in (b) denotes a 1D branch cut ending at the point defect. A line defect can act on both composite particles denoted by a black dot, and loops denoted by a red circle. Once a pointlike excitation and a loop excitation move around a line defect, the defect performs the Charles symmetry transformation Ω and W on the pointlike excitation and the loop excitation, respectively. In (b), the loop moves around the point defect such that the branch line intersects at the loop's spatial trajectory (a torus) only once. A Charles transformation induced by a point defect can only be $\mathcal{G} = W \oplus \Omega = \mathbb{I} \oplus \Omega$, which acts only on the loop excitations. However, due to Eq. (63), the only candidate for Ω is $\mathbb{I}$. This means that point defects can only behave like the identity element $\mathcal{G}_{\mathbb{I}}$ of Charles. Therefore, in 3D, we only consider line defects.

which is diagrammatically shown in Fig. 7(b). qp denotes pointlike particle excitations. $\mathcal{D}^0_{\mathcal{G}}$ denotes the bare line defect that is labeled by a Charles group element (or conjugacy class for a non-Abelian group) $\mathcal{G} = W \oplus \Omega$. qp_1 is any particle excitation provided by the parent 3D Abelian topological phase. Equation (72) means that the defect-charge composite $\mathcal{D}^0_{\mathcal{G}} \times qp$ is topologically equivalent to the defect-charge composite that is formed by the fusion between the same bare line defect and a different particle excitation given by $[qp + (\mathbb{I} - W)qp_1]$. Likewise, we have a similar equation for defect-loop composites:

$$\mathcal{D}^0_{\mathcal{G}} \times \text{loop} = \mathcal{D}^0_{\mathcal{G}} \times [\text{loop} + (\mathbb{I} - \Omega)\text{loop}_1], \tag{73}$$

which is diagrammatically shown in Fig. 7(c). One can also unify Eqs. (72) and (73) by considering charge-loop composites. We will show this in the following example.

Let us take $K = 3$ in Table III as an example. There is only one nontrivial group element given by $\mathcal{G} = -\mathbb{I} \oplus -\mathbb{I}$. For convenience, we label the three topologically distinct particle excitations as t_0, t_1, t_2 and the three distinct loop excitations as l_0, l_1, l_2. Using numerical labels, we have $t_0 = 0 \bmod 3$, $t_1 = 1 \bmod 3$, $t_2 = 2 \bmod 3$, and $l_0 = 0 \bmod 3$, $l_1 = 1 \bmod 3$, $l_2 = 2 \bmod 3$. We can consider the set of 2D vectors $\mathbf{V}_{ij} = (t_i, l_j)^T$ where $i, j = 0, 1, 2$ and hence, there are $3^2 = 9$ vectors that label the 9 topologically distinct charge-loop composites:

$$\{\mathbf{V}_{ij}\} = \begin{pmatrix}0\\0\end{pmatrix}, \begin{pmatrix}1\\0\end{pmatrix}, \begin{pmatrix}2\\0\end{pmatrix}, \begin{pmatrix}0\\1\end{pmatrix}, \begin{pmatrix}1\\1\end{pmatrix}, \begin{pmatrix}2\\1\end{pmatrix}, \begin{pmatrix}0\\2\end{pmatrix}, \begin{pmatrix}1\\2\end{pmatrix}, \begin{pmatrix}2\\2\end{pmatrix}.$$

As a result, Eqs. (72) and (73) can be unified as

$$\mathcal{D}^0_{\mathcal{G}} \times \mathbf{V} = \mathcal{D}^0_{\mathcal{G}} \times [\mathbf{V} + (\mathcal{G}_{\mathbb{I}} - \mathcal{G})\mathbf{V}'], \tag{74}$$

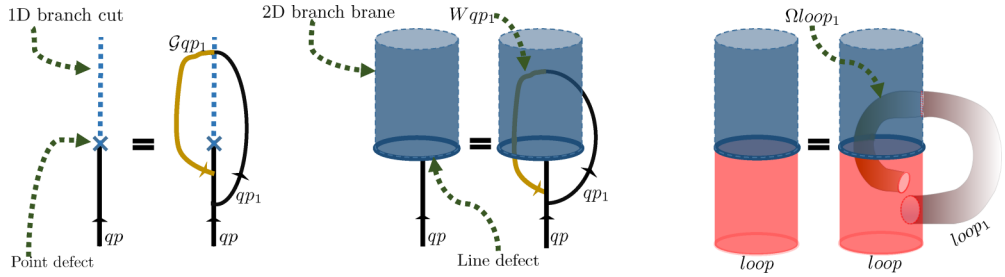

FIG. 7. Diagrammatic description of equivalence classes of fusion rules. (a) Shows the equivalent defect-anyon composites in 2D Abelian topological phases [74]. The bare point defect is labeled by a group element $\mathcal{G}$ of the anyonic symmetry group. The dashed lines are branch cuts that end at the defect. The vertical solid lines are quasiparticle (i.e., anyon, denoted by qp) strings (e.g., a string operator in the Wen-plaquette model), ending at the point defect. An anyon is transformed to another anyon when passing through the branch cut ($qp_1 \to \mathcal{G}qp_1$). The fusion of a bare defect denoted as $\mathcal{D}^0_{\mathcal{G}}$ and anyon (qp) forms a defect-anyon composite denoted as "$\mathcal{D}^0_{\mathcal{G}} \times qp$." It is topologically equivalent to the defect-anyon composite denoted as $\mathcal{D}^0_{\mathcal{G}} \times [qp + (\mathbb{I} - \mathcal{G})qp_1]$ where qp_1 denotes all anyons of the 2D Abelian topological phase. In 3D systems where Charles replaces the anyonic symmetry of 2D systems, (b) and (c) show line defects (denoted as solid blue circles) on which the 2D branch branes (denoted as the surface of a cylinder) terminate. By passing through the 2D branch branes, a particle and a loop are transformed to another particle and loop, respectively ($qp_1 \to Wqp_1$, $\text{loop}_1 \to \Omega\text{loop}_1$). In (b), the defect-charge (i.e., qp) composite denoted $\mathcal{D}^0_{\mathcal{G}} \times qp$ is topologically equivalent to $\mathcal{D}^0_{\mathcal{G}} \times [qp + (\mathbb{I} - W)qp_1]$ where qp_1 denotes all topologically distinct charge excitations. In (c), the red cylinder denotes the membrane operator that creates loop excitations and end on the line defect (the solid blue circles). The defect-loop composite denoted $\mathcal{D}^0_{\mathcal{G}} \times \text{loop}$ is topologically equivalent to $\mathcal{D}^0_{\mathcal{G}} \times [\text{loop} + (\mathbb{I} - \Omega)\text{loop}_1]$ where $\forall$ loop_1 denotes all topologically distinct loop excitations.

where $\mathbf{V}, \mathbf{V}' \in \{\mathbf{V}_{ij}\}$. By noting that $\mathcal{G}_{\mathbb{I}} - \mathcal{G} = \left(\begin{smallmatrix}1 & 0\\ 0 & 1\end{smallmatrix}\right) - \left(\begin{smallmatrix}-1 & 0\\ 0 & -1\end{smallmatrix}\right) = \left(\begin{smallmatrix}2 & 0\\ 0 & 2\end{smallmatrix}\right)$, the above relation reduces to

$$\mathcal{D}^0_{\mathcal{G}} \times \mathbf{V} = \mathcal{D}^0_{\mathcal{G}} \times (\mathbf{V} + 2\mathbf{V}'). \tag{75}$$

As a result, all defect-charge-loop composites are topologically equivalent to the bare defect $\mathcal{D}^0_{\mathcal{G}} = \mathcal{D}^0_{\mathcal{G}} \times \mathbf{V}_{ij}$, where $\{\mathbf{V}_{ij}\}$ denotes the nine vectors $(i,j = 0,1,2)$. The resulting fusion rules are given by

$$\mathbf{V}_{ij} \times \mathbf{V}_{i'j'} = \mathbf{V}_{(i+i')\text{mod}3,(j+j')\text{mod}3}\,, \tag{76}$$

$$\mathcal{D}^0_{\mathcal{G}} \times \mathcal{D}^0_{\mathcal{G}} = \sum_{ij} \mathbf{V}_{ij}, \tag{77}$$

from which we see that there are multiple fusion channels when two defects are fused together. It indicates that the externally imposed line defect $\mathcal{D}^0_{\mathcal{G}}$ is of non-Abelian nature.

V. CONCLUSIONS

In this work, a composite particle theory for 3D fermionic gapped phases was formulated based on a specific parton construction of electrons. Composite particles are bound states of partons and magnetic monopoles for a set of internal gauge fields and the external electromagnetic field A_μ. The resulting fully gapped phases were constructed by condensing two composite particles. All excitations including pointlike and stringlike excitations as a whole form a charge-loop lattice. Each site of the charge-loop lattice corresponds to a deconfined excitation of the condensed phase. A general mechanism for charge fractionalization in 3D was studied in detail. Based on the general framework of composite particle theory, we further explored two important properties of 3D Abelian topological phases. First, we studied phases with nonvanishing axion Θ angle which is characteristic of the tilted charge lattice. It was found that time-reversal-invariant fractional topological insulators with $\Theta \neq \pi$ can be constructed from composite particle theory. Second, we generalized the notion of anyonic symmetry of 2D Abelian topological phases to a charge-loop excitation permutation symmetry (Charles) group in 3D Abelian topological phases. We also investigated the relation between Charles group elements and line twist defects in (3+1)D Abelian topological phases.

There are several interesting directions for future studies. *First*, it is interesting to propose a systematic theory of the symmetric surface states of fractional topological insulators based on the composite particle theory. The 2D surface may exhibit quantum phenomena that are even more exotic than the surface topological order recently found on the surface of interacting topological insulators and interacting bosonic topological insulators [91,118–128]. For the FTI bulk lattice model construction and the phase diagram of confinement/deconfinement, the idea in Ref. [57] may be helpful. *Second*, one may consider the composite particle theory by assuming that partons form topological superconductor *Ansätze*, which may lead to interacting topological superconductors with fractional gravitoelectromagnetism and a fractional version of the gravitational Witten effect [129,130]. *Third*, as discussed in Sec. IV B, the tensor-network-type graphs may be helpful for understanding 3D analogs of the twist liquid, i.e., the topological phases obtained by gauging Charles. *Fourth*, it is interesting to think if there are simple 3D lattice models that can demonstrate the physics of extrinsic defects and Charles, in analogy to the 2D case where there are lattice models like the Wen-plaquette model. In addition, some group elements of Charles may break U(1) charge symmetry. A line defect associated with such a group element might be realized in a U(1)-symmetric 3D lattice model as an

extrinsic defect coated with a superconducting region. *Fifth*, in analogy to 2D anyonic symmetry where G-crossed tensor category theory [73,78] was proposed, a generic mathematical framework is also needed for 3D extrinsic defects. *Sixth*, it would be useful to have a microscopic theory of 3D line twist defects in terms of a cutting and gluing procedure where the twist defects are formed by tuning/twisting allowed tunneling terms between the two sides of a gapless cut [80–82,131].

ACKNOWLEDGMENTS

We would like to thank K. Shiozaki, Y. Qi, and S. Ryu for helpful discussions. P.Y. would like to thank Z.-Y. Weng and X.-G. Wen for beneficial collaborations and insightful discussions on parton constructions, and also acknowledges S.-T. Yau's hospitality at the Center of Mathematical Sciences and Applications at Harvard University where the work was done in part. This work was supported in part by the NSF through Grant No. DMR 1408713 at the University of Illinois (P.Y. and E.F.). T.L.H. is supported by the US National Science Foundation under Grant No. DMR 1351895-CAR. J.M. was supported by NSERC Grant No. RGPIN-2014-4608, the Canada Research Chair Program (CRC), the Canadian Institute for Advanced Research (CIFAR), and the University of Alberta.

APPENDIX A: SUMMARY OF NOTATIONS, ABBREVIATIONS, AND DEFINITIONS

In this Appendix, several notations, abbreviations, definitions, and criteria are collected for the reader's convenience.

1. Mathematical notations

u,v,u',v',q,q': a set of parameters that label the two condensed composites as shown in Table I.

Q: the net EM electric charge carried by a composite.

Q_{Debye}: the screening charge cloud around a composite. It is induced by the two composite condensates φ_1 and φ_2.

N_A: the bare EM electric charge carried by a composite. It is related to Q via Eqs. (28) and (29).

M: the EM magnetic charge carried by a composite.

M_μ: the 4-current of EM magnetic monopoles, introduced in Sec. III A.

$N_{a,b}$: gauge charges in $\mathrm{U}(1)_a$ and $\mathrm{U}(1)_b$ gauge groups. An integer vector $\mathbf{N}_e$ is formed via Eq. (15).

$N_m^{a,b}$: magnetic charges in $\mathrm{U}(1)_a$ and $\mathrm{U}(1)_b$ gauge groups. An integer vector $\mathbf{N}_m$ is formed via Eq. (14).

Γ: self-statistics of a composite. Γ is even (odd) if the composite is bosonic (fermionic) [see Eq. (11)].

θ: $\theta = 0$ if all partons (f^1, f^2, f^3) form trivial band insulators. $\theta = \pi$ if all partons form topological insulators.

ϑ^{cl}: the mutual statistics between a pointlike particle excitation and a loop excitation [see Eq. (34)].

Θ: the axion angle of the electron states (i.e., the resulting fermionic gapped phase constructed via the composite particle theory).

$g_{a,b}$: dimensionless gauge coupling constants of $\mathrm{U}(1)_{a,b}$ gauge groups.

$\mathcal{D}^0_{\mathcal{G}}$: a bare line defect associated with Charles group element $\mathcal{G}$.

2. Abbreviations

Charles: charge-loop excitation symmetry.

EM: electromagnetic (specific to the usual background electromagnetic field A_μ).

FQH: fractional quantum Hall effect.

FTI: fractional topological insulator.

GCD: greatest common divisor.

GSD: ground state degeneracy.

IQH: integer quantum Hall effect.

SET: symmetry-enriched topological phase.

SPT: symmetry-protected topological phase.

TI: free-fermion topological insulator.

TO: topological order.

TQFT: topological quantum field theory.

3. Definitions

Loop-lattice: Definition 1.

Excitation and charge lattice: Definition 2.

Intrinsic excitation and intrinsic charge lattice: Definition 3.

Charge-loop lattice: Definition 4.

Charge-loop excitation symmetry: Definition 5.

4. Others

Criterion 1 for loop excitations.

Criterion 2 for charge fractionalization.

Criterion 3 for charge fractionalization.

APPENDIX B: TECHNICAL DETAILS IN SEC. II

1. Details of Eq. (12)

By inserting the data of φ_1 and φ_2 in Table I into Eq. (10), one may obtain

$$\Gamma(\varphi_1) = 3q - \frac{\theta}{2\pi}[u(u+1)+v(v+1)+(u+v)(u+v-1)] \tag{B1}$$

and

$$\Gamma(\varphi_1) = 3q' - \frac{\theta}{2\pi}[u'(u'+1)+v'(v'+1) + (u'+v')(u'+v'-1)]. \tag{B2}$$

2. Proof of Theorem 1

We present Bézout's lemma as a preliminary [132]: Let a and b be nonzero integers and let d be their greatest common divisor (GCD). Then there exist integers x and y such that $ax + by = d$. In addition, d is the smallest positive integer that can be written as $ax + by$; every integer of the form $ax + by$ is a multiple of d.

Let us now prove Theorem 1.

Proof.

Sufficiency: When $|uv' - u'v| = 1$, according to Eq. (21), we straightforwardly obtain $|\mathrm{GCD}(u,u')| = 1, |\mathrm{GCD}(v,v')| = 1$. Then, the equalities in Eq. (21) hold. Therefore, $(\Phi_e^a)_{\min} = 2\pi$, $(\Phi_e^b)_{\min} = 2\pi$ in Eq. (20).

Necessity: We start with the equalities in Eq. (21), i.e., $|uv' - u'v| = |\mathrm{GCD}(u,u')| = |\mathrm{GCD}(v,v')|$. If $|uv' - u'v| \neq 1$, meaning that $|\mathrm{GCD}(u,u')| = |\mathrm{GCD}(v,v')| \neq 1$. Therefore,

u,u' are not coprime; v,v' are not coprime. Then, we consider

$$1 = \left| \frac{u}{\mathrm{GCD}(u,u')} v' - \frac{u'}{\mathrm{GCD}(u,u')} v \right| , \tag{B3}$$

where $\frac{u}{\mathrm{GCD}(u,u')}, \frac{u'}{\mathrm{GCD}(u,u')}$ are coprime by definition, i.e.,

$$\left| \mathrm{GCD}\left(\frac{u}{\mathrm{GCD}(u,u')}, \frac{u'}{\mathrm{GCD}(u,u')} \right) \right| = 1 .$$

Then, according to Eq. (21), we can also have the following inequalities if we just replace u and u' in Eq. (21) by $\frac{u}{\mathrm{GCD}(u,u')}$ and $\frac{u'}{\mathrm{GCD}(u,u')}$, respectively:

$$\left| \frac{u}{\mathrm{GCD}(u,u')} v' - \frac{u'}{\mathrm{GCD}(u,u')} v \right| \geqslant |\mathrm{GCD}(v,v')| . \tag{B4}$$

Due to Eqs. (B3) and (B4), we obtain $|\mathrm{GCD}(v,v')| = 1$. This is contradictory to our starting point $|\mathrm{GCD}(v,v')| \neq 1$. Therefore, the only possibility is $|uv' - u'v| = |\mathrm{Det}K| = 1$. ■

3. Equivalence between Criteria 2 and 3

Consider two excitations in a $\mathrm{U}(1)_{\mathrm{EM}}$-symmetric system. Let one carry zero EM magnetic charge $M = 0$ and minimal nonvanishing EM electric charge $Q = \frac{1}{w}$ with $w \in \mathbb{Z}$. Let the other excitation carry a minimal nonzero EM magnetic charge w' and an EM electric charge, say, y. y can be either integer or noninteger. Due to the Dirac-Zwanziger-Schwinger quantization condition [133–137], the magnetic and electric charges of the above two excitations satisfy

$$\left(\frac{1}{w} \times w' - 0 \times y \right) = 0, \quad \pm 1, \pm 2, \ldots . \tag{B5}$$

Therefore, the minimal choice of w' is $w' = w$, indicating that the change of quantization of the EM magnetic charge M is accompanied with a change of the charge quantization. Once $w > 1$, w' is also larger than one. In this sense, the two criteria are equivalent.

4. Debye-Hückel charge cloud Q_{Debye} is the unique source of charge fractionalization

In this Appendix, we prove that the Debye-Hückel charge cloud Q_{Debye} defined in Eq. (29) is the *unique* source of charge fractionalization. In other words, N_A is always integer valued when $M = 0$. By definition in Eqs. (2)–(4), N_A is given by

$$\begin{aligned} N_A &= N^{f1} + N^{f2} - N^{f3} \\ &= (n^{f1} + n^{f2} - n^{f3}) + \frac{3\theta}{2\pi} M - \frac{2\theta}{2\pi} N_m^b , \end{aligned} \tag{B6}$$

where n^{fi} are integer valued. N_m^b is integer valued, and $\theta = 0, \pi$. Therefore, $-\frac{2\theta}{2\pi} N_m^b$ is always integer valued. As a result, N_A is integer valued when $M = 0$.

APPENDIX C: TECHNICAL DETAILS IN SEC. III

1. Partons occupying trivial bands

We assume that all partons f^i (pure gauge charge carriers) form three trivial band insulators ($\theta = 0$). According to Eqs. (7), (8), and 12), we have

$$u,v,u',v' \in \mathbb{Z}; \quad q,q' \in \mathbb{Z}_{\mathrm{even}} . \tag{C1}$$

Since $\theta = 0$, we have

$$N^{fi} = n^{fi} \in \mathbb{Z} \tag{C2}$$

according to Eq. (4). Due to the definitions in Sec. II, we end up with

$$N_a, N_b \in \mathbb{Z} . \tag{C3}$$

Thus, in the mean-field *Ansätze* with $\theta = 0$, all magnetic charges and electric charges of composites are integer valued. However, Q_{Debye} and Q may be fractional, depending on the condensate parameters.

According to Definition 2, excitations are a subset of generic composites and satisfy the two equations in Eq. (23). Thus, only a 4D sublattice embedded in the 6D lattice survives, i.e., the charge lattice in Definition 2. Since $N_a (= N^{f1} - N^{f2})$ and $N_b (= N^{f3} - N^{f2})$ are fully determined by M via Eq. (24), we may use the labels $(N^{f2}, M, N_m^a, N_m^b)$. These four linearly independent integer numbers are "4D coordinates" of the 4D lattice that label excitations. Then, the bare EM electric charge N_A is expressed as

$$N_A = N^{f1} + N^{f2} - N^{f3} = (r - s)M + N^{f2} . \tag{C4}$$

The net EM electric charge Q is given by

$$\begin{aligned} Q &= N_A - Q_{\mathrm{Debye}} \\ &= N^{f1} + N^{f2} - N^{f3} - Q_{\mathrm{Debye}} \\ &= (r - s)M + N^{f2} - r N_m^a - s N_m^b , \end{aligned} \tag{C5}$$

where $N^{f1} - N^{f2} = rM$, $N^{f3} - N^{f2} = sM$ with r and s

$$r = \frac{qv' - q'v}{\mathrm{Det}K}, \quad s = \frac{q'u - qu'}{\mathrm{Det}K} . \tag{C6}$$

We note that r and s can be either integer or nonintegral rational numbers. However, rM and sM must be integer valued in order to ensure the N^{fi} are integer valued. Thus, the quantization of M should be altered properly if r and s are nonintegral rational numbers. In summary, we can define the following domains:

$$N^{f2} \in \mathbb{Z}, \quad N_m^a \in \mathbb{Z}, \quad N_m^b \in \mathbb{Z}, \quad \frac{M}{w} \in \mathbb{Z} , \tag{C7}$$

where w is a positive minimal integer such that both $rM \in \mathbb{Z}$ and $sM \in \mathbb{Z}$ are satisfied. In Eq. (C5), the M-dependent charge $(r - s)M$ is integer valued:

$$(r - s)M \in \mathbb{Z} . \tag{C8}$$

Therefore, the minimal quantized value of Q is sufficiently determined by rN_m^a and sN_m^b by noting that the latter two terms can be potentially fractionalized depending on r and s. In the language of the EM response theory, M-dependent charge means that the EM magnetic current minimally couples to the EM gauge field A_μ. In other words, the bulk supports an EM response action with Θ term. If we define $\frac{\Theta}{2\pi} M = (r - s)M$, then $Q = \frac{\Theta}{2\pi} M + N^{f2} - r N_m^a - s N_m^b$ with $\Theta = 2\pi(r - s)$. However, due to Eq. (C8), this nonzero Θ gives rise to an integer charge cloud surrounding EM magnetic monopoles. This additional charge cloud does not render a new

quantization of Q different from the quantization when $M = 0$. In other words, the EM charge lattice ($M - Q$ plane) is just a square lattice that is not tilted. The allowed values of Q when $M = 0$ are completely the same as when $M \neq 0$. In this sense, the resulting state with $\Theta = 2\pi(r - s)$ is equivalent to a trivial state with $\Theta = 0$. By comparison, a typical example with nontrivial Θ angle has a Q quantization shown in Eqs. (51) and (52) of Sec. III B where the quantization of Q manifestly depends on M.

2. Derivation of Eqs. (51), (52), and (58), and the site distribution in Fig. 5(c)

Since M is quantized in multiples of 3 as indicated in Eq. (45), one may introduce an integer k such that $M = 3k$. Meanwhile, Eq. (50) indicates that Q is generically quantized in multiples of $\frac{1}{6}$. Thus, we can introduce an integer k_0 such that $Q = \frac{k_0}{6}$. Then, Eq. (50) is formulated as

$$k_0 + 5k = 2(7n^{f1} - n^{f2} - 3n^{f3}), \tag{C9}$$

where the right-hand side is always even. $5k$ has the same even-odd property as k. As a result, k_0 and k must be simultaneously either odd or even, which leads to Eqs. (51) and (52).

Then, we start with Γ in Eq. (53) and derive its equivalent expression (58). Due to Eqs. (45) and (52), we introduce four integer numbers k_0,k_1,k_2,k_3 via

$$M = 3k, \quad N_m^a = 2k_1, \quad N_m^b = 2k_2, \quad Q = \frac{k_0}{6} \tag{C10}$$

so as to simplify the analysis below. Then, solving Eqs. (46), (47), and (50) leads to

$$n^{f1} = -\frac{5}{2}k + \frac{k_0}{6} + \frac{5}{3}k_1 - \frac{2}{3}k_2, \tag{C11}$$

$$n^{f2} = -\frac{13}{2}k + \frac{k_0}{6} + \frac{11}{3}k_1 + \frac{1}{3}k_2, \tag{C12}$$

$$n^{f3} = -\frac{9}{2}k + \frac{k_0}{6} + \frac{8}{3}k_1 - \frac{5}{3}k_2. \tag{C13}$$

Therefore, Γ in Eq. (58) can be reformulated as

$$\Gamma = (M+1)\left(-14k + \frac{1}{2}k + \frac{k_0}{2} + 8k_1 - 2k_2\right). \tag{C14}$$

Since $(M+1)(-14k + 8k_1 - 2k_2)$ is always an even integer, we may remove it and end up with

$$\Gamma = (M+1)\left(\frac{1}{2}k + \frac{k_0}{2}\right) = 3(M+1)\left(Q + \frac{1}{18}M\right) \tag{C15}$$

which can be rewritten as

$$\Gamma = 3(M+1)\left(Q - \frac{\Theta}{2\pi}M\right) \tag{C16}$$

with $\Theta = -\frac{1}{9}\pi$. One can check that Γ is invariant under the shift $\Theta \to \Theta + \frac{2}{9}\pi$ since the additional term $-3(M+1)\frac{1}{9}M = -k(3k+1)$ is always an even integer which leaves the even/odd property of Γ unaltered. From this point of view, we say that two Θ's are topologically equivalent if their difference is given by multiples of $\frac{2}{9}\pi$. In conclusion,

$$\Theta = \tfrac{1}{9}\pi \bmod \tfrac{2}{9}\pi\,. \tag{C17}$$

As a result, $-\frac{1}{9}\pi$, $\frac{1}{9}\pi$, $-\frac{5}{9}\pi$, etc., describe the same FTI states. The periodicity $\frac{2}{9}\pi$ is the minimal one in the sense that any shift smaller than $\frac{2}{9}\pi$ does not keep the even-odd property of Γ invariant. In other words, the charge lattice with "tilt angle" $\Theta = \frac{1}{9}\pi$ is always different from a lattice with $\Theta = 0$. This periodicity check is very important since it is possible that a nonzero Θ might be entirely removed by a periodic shift. If this happens, the resulting bulk state is actually a trivial state.

Next, we calculate the lattice sites in Fig. 5(b). Since $Q = \frac{1}{6}$ and $M = 3$, we have $k_0 = 1$, $k = 1$:

$$n^{f1} = (-2 + 2k_1 - k_2) + \frac{-1 - k_1 + k_2}{3}, \tag{C18}$$

$$n^{f2} = (-6 + 4k_1) + \frac{-1 - k_1 + k_2}{3}, \tag{C19}$$

$$n^{f3} = (-4 + 3k_1 - 2k_2) + \frac{-1 - k_1 + k_2}{3}. \tag{C20}$$

Therefore, $-1 - k_1 + k_2$ should be quantized in multiples of 3 such that the n^{fi}'s are integer valued. By noting that $N_m^a = 2k_1$, $N_m^b = 2k_2$, we end up with Fig. 5(c) where $k_0 = 1$, $k = 0$ are assumed.

APPENDIX D: TECHNICAL DETAILS IN ESC. IV

1. Charles is a group

Proof. Step 1 is to prove that Auto(K) is a group. In other words, the elements satisfy the four group axioms (identity element, inverse element, closure, associativity).

Identity element: The identity element is $\mathcal{G}_{\mathbb{I}} = W \oplus \Omega = \mathbb{I} \oplus \mathbb{I}$ where $\mathbb{I}$ is a rank-2 identity matrix. For every element $\mathcal{G}$ in Auto(K), the equation $\mathcal{G} \cdot \mathcal{G}_{\mathbb{I}} = \mathcal{G}_{\mathbb{I}} \cdot \mathcal{G} = \mathcal{G}$ holds. Here, the symbol $\cdot$ denotes matrix multiplication. We will also omit it unless otherwise specified.

Associativity: Associativity is guaranteed by matrix multiplication rules.

Inverse element: The inverse element of $\mathcal{G}$ is given by $\mathcal{G}^{-1} = W^{-1} \oplus \Omega^{-1}$. One may check that $(W^{-1} \oplus \Omega^{-1}) \cdot (W \oplus \Omega) = \mathbb{I} \oplus \mathbb{I} = \mathcal{G}_{\mathbb{I}}$ and $(W \oplus \Omega) \cdot (W^{-1} \oplus \Omega^{-1}) = \mathcal{G}_{\mathbb{I}}$, which means that $\mathcal{G}^{-1} \cdot \mathcal{G} = \mathcal{G} \cdot \mathcal{G}^{-1} = \mathcal{G}_{\mathbb{I}}$.

Closure: Suppose $\mathcal{G}' = W' \oplus \Omega' \in$ Auto(K). Thus, W,Ω,W',Ω' matrices satisfy conditions (i) and (ii) in Definition 5. Then, by definition, $\mathcal{G}' \cdot \mathcal{G} = (W'W) \oplus (\Omega'\Omega)$. Both $W'W$ and $\Omega'\Omega$ are still rank-2 unimodular matrices. Furthermore,

$$(\Omega'\Omega)K(W'W)^T = \Omega'(\Omega K W^T)W'^T = \Omega' K W'^T = K\,.$$

Therefore, condition (i) is satisfied. And,

$$\begin{aligned}\Gamma[\ldots,&(W'W)^{-1}\mathbf{N}_m,\ldots] \\ &= \Gamma(\ldots, W^{-1}W'^{-1}\mathbf{N}_m,\ldots) \\ &= \Gamma(\ldots, W'^{-1}\mathbf{N}_m,\ldots) \\ &= \Gamma(\ldots,\mathbf{N}_m,\ldots)\,.\end{aligned}$$

Therefore, condition (ii) is also satisfied.

Step 2 is to verify that Inner(K) is a subgroup of Auto(K). First, it is a subset of Auto(K), i.e., Inner(K) $\subset$ Auto(K) since not only do W and Ω satisfy conditions (i) and (ii), but also

satisfy

$$W^{-1}\mathbf{N}_m - \mathbf{N}_m = K^T (n_1,n_2)^T \tag{D1}$$

and

$$\Omega^{-1}\mathbf{L} - \mathbf{L} = K(n_3,n_4)^T . \tag{D2}$$

Here, $n_1,\ldots,n_4$ are integers. n_1,n_2 depend on $\mathbf{N}_m, W$; n_3,n_4 depend on $\mathbf{L},\Omega$.

$\mathcal{G}_{\mathbb{I}} \in \text{Inner}(K)$ since one can obtain $\mathcal{G}_{\mathbb{I}}\mathbf{L} - \mathbf{L} = 0$ and $\mathcal{G}_{\mathbb{I}}\mathbf{N}_m - \mathbf{N}_m = 0$ by choosing $n_1 = n_2 = n_3 = n_4 = 0$ for all $\mathbf{L}$'s and $\mathbf{N}_m$'s. Then, elements of Inner(K) have associativity arising from the standard matrix multiplication.

For the existence of the inverse element, we need to prove that $W^{-1} \oplus \Omega^{-1} \in \text{Inner}(K)$. By definition, for $W \oplus \Omega \in \text{Inner}(K)$, the operation of W is

$$W^{-1}\mathbf{N}_m - \mathbf{N}_m = K^T \mathbf{J}_{W,\mathbf{N}_m},$$

where the notation $\mathbf{J}_{W,\mathbf{N}_m}$ denotes the integer vector $(n_1,n_2)^T$ and the subscript $W,\mathbf{N}_m$ means that the integer vector is a function of W and $\mathbf{N}_m$. Likewise, we also have

$$W^{-1}(W\mathbf{N}_m) - W\mathbf{N}_m = K^T \mathbf{J}_{W,W\mathbf{N}_m}.$$

As a result, $W\mathbf{N}_m - \mathbf{N}_m = -K^T \mathbf{J}_{W,W\mathbf{N}_m}$. Since $-\mathbf{J}_{W,W\mathbf{N}_m}$ is an integer vector, we obtain the operation of W^{-1}:

$$(W^{-1})^{-1}\mathbf{N}_m - \mathbf{N}_m = K^T(-\mathbf{J}_{W,W\mathbf{N}_m})$$

which exactly satisfies the defining property of Inner(K). Likewise, we can also prove that Ω^{-1} is an operation in Inner(K). Therefore, the inverse element $\mathcal{G}^{-1} = W^{-1} \oplus \Omega^{-1} \in \text{Inner}(K)$.

For the closure property, we need to prove that $\mathcal{G}' \cdot \mathcal{G} \in \text{Inner}(K)$ if $\mathcal{G}' \in \text{Inner}(K)$ and $\mathcal{G} \in \text{Inner}(K)$. For this purpose, let us calculate

$$\begin{aligned}
&(W'W)^{-1}\mathbf{N}_m - \mathbf{N}_m \\
&\quad = W^{-1}W'^{-1}\mathbf{N}_m - \mathbf{N}_m = W^{-1}\left(\mathbf{N}_m + K^T\mathbf{J}_{W',\mathbf{N}_m}\right) - \mathbf{N}_m \\
&\quad = (W^{-1}\mathbf{N}_m - \mathbf{N}_m) + W^{-1}K^T\mathbf{J}_{W',\mathbf{N}_m} \\
&\quad = K^T\mathbf{J}_{W,\mathbf{N}_m} + K^T\Omega^T\mathbf{J}_{W',\mathbf{N}_m} = K^T\left(\mathbf{J}_{W,\mathbf{N}_m} + \Omega^T\mathbf{J}_{W',\mathbf{N}_m}\right),
\end{aligned}$$

where we have used $W^{-1}K^T = K^T\Omega^T$ that is an equivalent expression of condition (i). Since $\mathbf{J}_{W,\mathbf{N}_m} + \Omega^T\mathbf{J}_{W',\mathbf{N}_m}$ is an integer vector (by noting that Ω is unimodular), we conclude that $W'W$ satisfies the defining property of Inner(K). So does $\Omega\Omega'$. Therefore, $\mathcal{G}' \cdot \mathcal{G} \in \text{Inner}(K)$.

Step 3 is to prove that Inner(K) is normal. In other words, we need to verify that $W'WW'^{-1} \in \text{Inner}(K)$ and $\Omega'\Omega\Omega'^{-1} \in \text{Inner}(K)$ for $\forall\ W,\Omega \in \text{Inner}(K)$ and $\forall\ W',\Omega' \in \text{Auto}(K)$. For this purpose, let us calculate

$$\begin{aligned}
&(W'WW'^{-1})^{-1}\mathbf{N}_m - \mathbf{N}_m \\
&\quad = W'(W^{-1}W'^{-1}\mathbf{N}_m) - \mathbf{N}_m \\
&\quad = W'\left(W'^{-1}\mathbf{N}_m + K^T\mathbf{J}_{W,W'^{-1}\mathbf{N}_m}\right) - \mathbf{N}_m \\
&\quad = W'K^T\mathbf{J}_{W,W'^{-1}\mathbf{N}_m}.
\end{aligned}$$

Since $W' \in \text{Auto}(K)$, condition (i) in Eq. (63) leads to $\Omega'KW'^T = K$, and thereby $W'K^T\Omega'^T = K^T$. Therefore, $W'K^T = K^T(\Omega'^T)^{-1}$. Therefore,

$$(W'WW'^{-1})^{-1}\mathbf{N}_m - \mathbf{N}_m = K(\Omega'^T)^{-1}\mathbf{J}_{W,W'^{-1}\mathbf{N}_m}.$$

Since $(\Omega'^T)^{-1}$ is obviously a unimodular matrix, it implies that $(\Omega'^T)^{-1}\mathbf{J}_{W,W'^{-1}\mathbf{N}_m}$ is an integer vector. Thus, by the definition of Inner(K), $W'WW'^{-1} \in \text{Inner}(K)$. Likewise, we also have $\Omega'\Omega\Omega'^{-1} \in \text{Inner}(K)$. Therefore, we conclude that Inner(K) is a normal subgroup of Auto(K).

Then, according to the definition of Charles, the elements of Charles form a quotient group of Auto(K) by Inner(K). It can be non-Abelian since $\mathcal{G} \cdot \mathcal{G}' \neq \mathcal{G}' \cdot \mathcal{G}$ may hold for some elements. ■

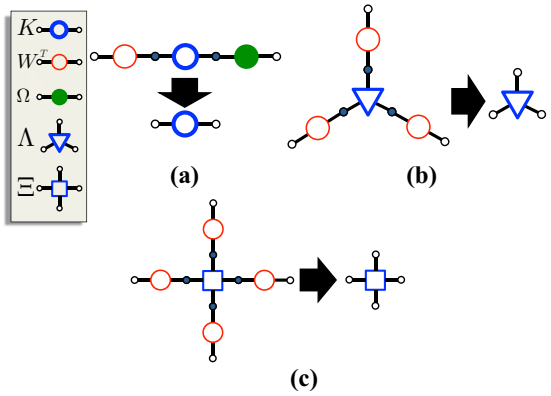

FIG. 8. Tensor-network-type graphical representations of Charles transformations. (a) Represents Eq. (63) where K is a fixed-point matrix. (b) Represents Eq. (68) where Λ is a fixed-point tensor with a bond dimension no less than two. (c) Represents Eq. (70) where Ξ is a fixed-point tensor with a bond dimension no less than four.

2. Graphical representations of Charles transformations

Equations (63), (68), and (70) are graphically represented in Fig. 8 where a tensor-network-type graph is introduced.

[1] K. v. Klitzing, G. Dorda, and M. Pepper, Phys. Rev. Lett. **45**, 494 (1980).
[2] F. D. M. Haldane, Phys. Rev. Lett. **61**, 2015 (1988).
[3] J. E. Moore and L. Balents, Phys. Rev. B **75**, 121306 (2007).
[4] L. Fu, C. L. Kane, and E. J. Mele, Phys. Rev. Lett. **98**, 106803 (2007).
[5] R. Roy, Phys. Rev. B **79**, 195322 (2009).
[6] M. Z. Hasan and C. L. Kane, Rev. Mod. Phys. **82**, 3045 (2010).
[7] J. E. Moore, Nature (London) **464**, 194 (2010).
[8] X.-L. Qi and S.-C. Zhang, Rev. Mod. Phys. **83**, 1057 (2011).
[9] Y. Xia, D. Qian, D. Hsieh, L. Wray, A. Pal, H. Lin, A. Bansil, D. Grauer, Y. Hor, R. Cava, and M. Z. Hasan, Nat. Phys. **5**, 398 (2009).
[10] G. Baskaran, Z. Zou, and P. Anderson, Solid State Commun. **63**, 973 (1987).
[11] G. Baskaran and P. W. Anderson, Phys. Rev. B **37**, 580 (1988).

[12] I. Affleck and J. B. Marston, Phys. Rev. B **37**, 3774 (1988).
[13] G. Kotliar and J. Liu, Phys. Rev. B **38**, 5142 (1988).
[14] Y. Suzumura, Y. Hasegawa, and H. Fukuyama, J. Phys. Soc. Jpn. **57**, 2768 (1988).
[15] I. Affleck, Z. Zou, T. Hsu, and P. W. Anderson, Phys. Rev. B **38**, 745 (1988).
[16] E. Dagotto, E. Fradkin, and A. Moreo, Phys. Rev. B **38**, 2926 (1988).
[17] X.-G. Wen, F. Wilczek, and A. Zee, Phys. Rev. B **39**, 11413 (1989).
[18] X.-G. Wen, Phys. Rev. B **44**, 2664 (1991).
[19] P. A. Lee and N. Nagaosa, Phys. Rev. B **46**, 5621 (1992).
[20] C. Mudry and E. Fradkin, Phys. Rev. B **49**, 5200 (1994).
[21] X.-G. Wen and P. A. Lee, Phys. Rev. Lett. **76**, 503 (1996).
[22] P. A. Lee, N. Nagaosa, and X.-G. Wen, Rev. Mod. Phys. **78**, 17 (2006).
[23] Z. Y. Weng, D. N. Sheng, Y.-C. Chen, and C. S. Ting, Phys. Rev. B **55**, 3894 (1997).
[24] P. Ye, C.-S. Tian, X.-L. Qi, and Z.-Y. Weng, Phys. Rev. Lett. **106**, 147002 (2011).
[25] P. Ye, C.-S. Tian, X.-L. Qi, and Z.-Y. Weng, Nucl. Phys. B **854**, 815 (2012).
[26] P. Ye, L. Zhang, and Z.-Y. Weng, Phys. Rev. B **85**, 205142 (2012).
[27] Y. Ma, P. Ye, and Z.-Y. Weng, New J. Phys. **16**, 083039 (2014).
[28] P. Ye and Q.-R. Wang, Nucl. Phys. B **874**, 386 (2013).
[29] J. K. Jain, Phys. Rev. B **40**, 8079 (1989).
[30] X.-G. Wen, Mod. Phys. Lett. B **05**, 39 (1991).
[31] X.-G. Wen, Phys. Rev. B **60**, 8827 (1999).
[32] M. Barkeshli and X.-G. Wen, Phys. Rev. B **81**, 155302 (2010).
[33] Y.-M. Lu and D.-H. Lee, Phys. Rev. B **89**, 184417 (2014).
[34] P. Ye and X.-G. Wen, Phys. Rev. B **87**, 195128 (2013).
[35] P. Ye and X.-G. Wen, Phys. Rev. B **89**, 045127 (2014).
[36] C. Wang, A. Nahum, and T. Senthil, Phys. Rev. B **91**, 195131 (2015).
[37] Z.-X. Liu, J.-W. Mei, P. Ye, and X.-G. Wen, Phys. Rev. B **90**, 235146 (2014).
[38] Z.-C. Gu and X.-G. Wen, Phys. Rev. B **80**, 155131 (2009).
[39] X. Chen, Z.-C. Gu, Z.-X. Liu, and X.-G. Wen, Phys. Rev. B **87**, 155114 (2013).
[40] X. Chen, Z.-C. Gu, Z.-X. Liu, and X.-G. Wen, Science **338**, 1604 (2012).
[41] X. Chen, Z.-C. Gu, and X.-G. Wen, Phys. Rev. B **82**, 155138 (2010).
[42] G. 't Hooft, Nucl. Phys. B **190**, 455 (1981).
[43] S. Deser, R. Jackiw, and S. Templeton, Ann. Phys. (NY) **140**, 372 (1982).
[44] S. Mandelstam, Phys. Rep. **67**, 109 (1980).
[45] M. E. Peskin, Ann. Phys. (NY) **113**, 122 (1978).
[46] A. M. Polyakov, Phys. Lett. B **59**, 82 (1975).
[47] A. M. Polyakov, Nucl. Phys. B **120**, 429 (1977).
[48] A. M. Polyakov, Phys. Lett. B **72**, 477 (1978).
[49] G. 't Hooft, Nucl. Phys. B **138**, 1 (1978).
[50] G. 't Hooft, Nucl. Phys. B **153**, 141 (1979).
[51] L. Susskind, Phys. Rev. D **20**, 2610 (1979).
[52] E. Fradkin and L. Susskind, Phys. Rev. D **17**, 2637 (1978).
[53] *Confinement, Duality, and Nonperturbative Aspects of QCD*, edited by P. van Baal (Kluwer Academic, Dordrecht, 2002).
[54] N. Seiberg and E. Witten, Nucl. Phys. B **431**, 484 (1994).
[55] O. Aharony, N. Seiberg, and Y. Tachikawa, J. High Energy Phys. 08 (2013) 115.
[56] F. A. Bais and J. K. Slingerland, Phys. Rev. B **79**, 045316 (2009).
[57] C. W. von Keyserlingk and F. J. Burnell, Phys. Rev. B **91**, 045134 (2015).
[58] E. Witten, Phys. Lett. B **86**, 283 (1979).
[59] X.-L. Qi, T. L. Hughes, and S.-C. Zhang, Phys. Rev. B **78**, 195424 (2008).
[60] J. K. Jain, Phys. Rev. Lett. **63**, 199 (1989).
[61] J. K. Jain, *Composite Fermions* (Cambridge University Press, Cambridge, 2007).
[62] A. Lopez and E. Fradkin, Phys. Rev. B **44**, 5246 (1991).
[63] B. I. Halperin, P. A. Lee, and N. Read, Phys. Rev. B **47**, 7312 (1993).
[64] R. Shankar and G. Murthy, Phys. Rev. Lett. **79**, 4437 (1997).
[65] B. I. Halperin, Phys. E (Amsterdam) **20**, 71 (2003).
[66] G. Murthy and R. Shankar, Rev. Mod. Phys. **75**, 1101 (2003).
[67] G. Rosenberg and M. Franz, Phys. Rev. B **82**, 035105 (2010).
[68] J. Maciejko, X.-L. Qi, A. Karch, and S.-C. Zhang, Phys. Rev. Lett. **105**, 246809 (2010).
[69] J. Maciejko, X.-L. Qi, A. Karch, and S.-C. Zhang, Phys. Rev. B **86**, 235128 (2012).
[70] J. Maciejko and G. A. Fiete, Nat. Phys. **11**, 385 (2015).
[71] B. Swingle, M. Barkeshli, J. McGreevy, and T. Senthil, Phys. Rev. B **83**, 195139 (2011).
[72] B. Swingle, Phys. Rev. B **86**, 245111 (2012).
[73] J. C. Teo, T. L. Hughes, and E. Fradkin, Ann. Phys. (NY) **360**, 349 (2015).
[74] M. N. Khan, J. C. Y. Teo, and T. L. Hughes, Phys. Rev. B **90**, 235149 (2014).
[75] A. Mesaros, Y. B. Kim, and Y. Ran, Phys. Rev. B **88**, 035141 (2013).
[76] M. Barkeshli and X.-G. Wen, Phys. Rev. B **81**, 045323 (2010).
[77] J. C. Y. Teo, A. Roy, and X. Chen, Phys. Rev. B **90**, 155111 (2014).
[78] M. Barkeshli, P. Bonderson, M. Cheng, and Z. Wang, arXiv:1410.4540.
[79] Y.-Z. You and X.-G. Wen, Phys. Rev. B **86**, 161107 (2012).
[80] M. Barkeshli and X.-L. Qi, Phys. Rev. X **2**, 031013 (2012).
[81] M. Barkeshli, C.-M. Jian, and X.-L. Qi, Phys. Rev. B **87**, 045130 (2013).
[82] M. Barkeshli and X.-L. Qi, Phys. Rev. X **4**, 041035 (2014).
[83] M. Barkeshli, H.-C. Jiang, R. Thomale, and X.-L. Qi, Phys. Rev. Lett. **114**, 026401 (2015).
[84] H. Bombin, Phys. Rev. Lett. **105**, 030403 (2010).
[85] J. L. Cardy and E. Rabinovici, Nucl. Phys. B **205**, 1 (1982).
[86] J. L. Cardy, Nucl. Phys. B **205**, 17 (1982).
[87] A. S. Goldhaber, R. MacKenzie, and F. Wilczek, Mod. Phys. Lett. A **04**, 21 (1989).
[88] G. T. Horowitz, Commun. Math. Phys. **125**, 417 (1989).
[89] R. Savit, Rev. Mod. Phys. **52**, 453 (1980).
[90] P. Ye and J. Wang, Phys. Rev. B **88**, 235109 (2013).
[91] M. A. Metlitski, C. L. Kane, and M. P. A. Fisher, Phys. Rev. B **88**, 035131 (2013).
[92] L. Kong and X.-G. Wen, arXiv:1405.5858.
[93] X.-G. Wen, Natl. Sci. Rev. **3**, 68 (2016).
[94] X.-G. Wen, Phys. Rev. Lett. **90**, 016803 (2003).
[95] A. Kitaev, Ann. Phys. (NY) **321**, 2 (2006).

[96] J. Cano, M. Cheng, M. Mulligan, C. Nayak, E. Plamadeala, and J. Yard, Phys. Rev. B **89**, 115116 (2014).
[97] M. Blau and G. Thompson, Ann. Phys. (NY) **205**, 130 (1991).
[98] M. Bergeron, G. W. Semenoff, and R. J. Szabo, Nucl. Phys. B **437**, 695 (1995).
[99] R. J. Szabo, Nucl. Phys. B **531**, 525 (1998).
[100] H. v. Bodecker and G. Hornig, Phys. Rev. Lett. **92**, 030406 (2004).
[101] R. Dijkgraaf and E. Witten, Commun. Math. Phys. **129**, 393 (1990).
[102] A. Kapustin and R. Thorngren, arXiv:1404.3230.
[103] P. Ye and Z.-C. Gu, Phys. Rev. B **93**, 205157 (2016).
[104] C. Wang and M. Levin, Phys. Rev. Lett. **113**, 080403 (2014).
[105] C. Wang and M. Levin, Phys. Rev. B **91**, 165119 (2015).
[106] C.-H. Lin and M. Levin, Phys. Rev. B **92**, 035115 (2015).
[107] X. Chen, A. Tiwari, and S. Ryu, Phys. Rev. B **94**, 045113 (2016).
[108] M. A. Levin and X.-G. Wen, Phys. Rev. B **71**, 045110 (2005).
[109] M. Levin and X.-G. Wen, Rev. Mod. Phys. **77**, 871 (2005).
[110] A. Hamma, P. Zanardi, and X.-G. Wen, Phys. Rev. B **72**, 035307 (2005).
[111] H. Moradi and X.-G. Wen, Phys. Rev. B **91**, 075114 (2015).
[112] J. C. Wang and X.-G. Wen, Phys. Rev. B **91**, 035134 (2015).
[113] S. Jiang, A. Mesaros, and Y. Ran, Phys. Rev. X **4**, 031048 (2014).
[114] Y. Wan, J. C. Wang, and H. He, Phys. Rev. B **92**, 045101 (2015).
[115] D. Gaiotto, A. Kapustin, N. Seiberg, and B. Willett, J. High Energy Phys. 02 (2015) 172.
[116] T. Iadecola, T. Neupert, C. Chamon, and C. Mudry, Phys. Rev. B **93**, 195136 (2016).
[117] J. Wang, X.-G. Wen, and S.-T. Yau, arXiv:1602.05951.
[118] A. Vishwanath and T. Senthil, Phys. Rev. X **3**, 011016 (2013).
[119] P. Ye and Z.-C. Gu, Phys. Rev. X **5**, 021029 (2015).
[120] C. Wang and T. Senthil, Phys. Rev. B **87**, 235122 (2013).
[121] C. Xu and T. Senthil, Phys. Rev. B **87**, 174412 (2013).
[122] S. D. Geraedts and O. I. Motrunich, Phys. Rev. X **4**, 041049 (2014).
[123] A. Kapustin, arXiv:1404.6659.
[124] X. Chen, L. Fidkowski, and A. Vishwanath, Phys. Rev. B **89**, 165132 (2014).
[125] C. Wang, A. C. Potter, and T. Senthil, Science **343**, 629 (2014).
[126] P. Bonderson, C. Nayak, and X.-L. Qi, J. Stat. Mech. (2013) P09016.
[127] M. A. Metlitski, C. L. Kane, and M. P. A. Fisher, Phys. Rev. B **92**, 125111 (2015).
[128] C. Wang, A. C. Potter, and T. Senthil, Phys. Rev. B **88**, 115137 (2013).
[129] S. Ryu, J. E. Moore, and A. W. W. Ludwig, Phys. Rev. B **85**, 045104 (2012).
[130] Z. Wang, X.-L. Qi, and S.-C. Zhang, Phys. Rev. B **84**, 014527 (2011).
[131] D.-H. Lee, G.-M. Zhang, and T. Xiang, Phys. Rev. Lett. **99**, 196805 (2007).
[132] G. A. Jones and J. M. Jones, *Elementary Number Theory* (Springer, London, 1998).
[133] P. A. Dirac, Proc. R. Soc. London, Ser. A **133**, 60 (1931).
[134] D. Zwanziger, Phys. Rev. **176**, 1480 (1968).
[135] D. Zwanziger, Phys. Rev. **176**, 1489 (1968).
[136] J. Schwinger, Phys. Rev. **144**, 1087 (1966).
[137] J. Schwinger, Phys. Rev. **173**, 1536 (1968).